Removal of antibiotics from wastewater using green synthesized iron oxide nanoparticles

By

Sikandar Altaf

00000273409

A thesis submitted in partial fulfillment of the requirements for the degree of

Master of Science

in

Environmental Science

Institute of Environmental Sciences and Engineering (IESE)

School of Civil and Environmental Engineering (SCEE)

National University of Sciences and Technology (NUST)

Islamabad, Pakistan

(2021)

Certificate

This is certified that the contents and form of the thesis entitled "**Removal of antibiotics from wastewater using green synthesized iron oxide nanoparticles**" submitted by Mr. Sikandar Altaf, Registration No. 00000273409, has been found satisfactory for the fulfillment of partial requirements of the degree of Master of Science in Environmental Science.

Supervisor: _____

Dr. Muhammad Arshad
Associate Professor
IESE, SCEE, NUST, Islamabad

GEC members: _____

Dr. Imran Hashmi
Professor,
IESE, SCEE, NUST, Islamabad

_____

Dr. Zeshan
Assistant Professor
IESE, SCEE, NUST, Islamabad

THESIS ACCEPTANCE CERTIFICATE

Certified that final copy of MS thesis written by **Mr. Sikandar Altaf** (Registration No. 00000273409) of **IESE (SCEE)** has been vetted by undersigned, found complete in all aspects as per NUST Statutes/Regulations, is free of plagiarism, errors and mistakes and is accepted as partial fulfilment for award of MS Degree. It is further certified that necessary amendments as pointed out by GEC members of the scholar have also been incorporated in the said thesis.

Signature: _____

Name of Supervisor: Dr Muhammad Arshad

Date: _____

Signature of HoD: _____

Date: _____

Countersigned by

Signature (Dean/ Principal): _____

Date: _____

Dedication

To my parents who inspired me to do it

Acknowledgements

I would like to express my utmost gratitude to **Allah Almighty**, the "Most Kind" and "Most Merciful" who blessed me with aptitude, skills, and wisdom to accomplish this project.

I would like to express my sincere appreciation to my supervisor, **Dr. Muhammad Arshad** for his guidance throughout this research work. His patience, support and motivation were as source of inspiration during the study. I am thankful to Guidance and Examination committee members **Dr. Imran Hashmi** and **Dr. Zeshan** for their constructive comments during this project. I am grateful to **Miss Rabeea Zafar** for her continuous guidance, support and giving me skills of HPLC as senior PhD student.

I would like to show special gratitude to my parents **Mr. Altaf Hussain and Mrs. Zarina Musarat** for their prayers, continuous support, and always been a source of encouragement.

My special thanks go to my friends **Haris Mashood** and **Samra Rehman Jami** who have provided welcome distraction, stress relief, encouragement, and bears me throughout my MS.

I am thankful to my family especially my Uncle **Aashiq Hussain**, elder brother and sister **Aamir Altaf** and **Rubina Altaf** for their guidance and encouragement.

I would like to extend my gratitude to **Environmental Biotechnology Research Group** for their help and support and all the labs in IESE (SCEE), NUST for providing the facilities like equipment and apparatus necessary for my research. The assistance of Lab Demonstrator **Miss. Anisa Tahir** for purchasing of chemicals, service of HPLC and other lab things was vital for completion of my work.

I would also like to thank **Hashir Muneeb** for providing *Moringa olifera* leaves for my research work. I also want to say thanks to my friends **Afnan Yasir**, **Mahnoor Ali**, **Muneeb Hassan** and other IESE fellows for their moral support and help in this study.

Last but not the least I would like to thank all the laboratory staff at IESE, and SCME NUST for their help and cooperation.

Sikandar Altaf

TABLE OF CONTENTS

List of Tables

List of Figures

List of Abbreviations

ABBREVIATION	ACRONYMS
WHO	World Health Organization
DDD	Defined Daily Doses
ECs	Emerging Contaminants
PCPs	Personal Care Products
m^3	Meter cube
COD	Chemical Oxygen Demand
mg/L	Milli gram per Liter
µg/L	Microgram per Liter
%	Percent
$	Dollar
AB	Antibiotics
°C	Degree Celsius
ng/L	Nanogram per Liter
Levo	Levofloxacin
M	Molar
g	gram
rpm	Revolution per minuet
mA	Milli Ampere
KV	Kilo volt
h	hour
nm	nanometer
FWHM	Full Width Half Maximum
cm^{-1}	Per centimeter
S. D	Standard Deviation
C-N	Carbon-Nitrogen

Abstract

The present study focused on green method of magnetite (Fe_3O_4) synthesis and its efficiency for removal of levofloxacin. The removal of levofloxacin onto the surface of green synthesized iron oxide nanoparticles (gINPs) was investigated in terms of adsorption capacity and removal efficiency for adsorbent dosage, adsorbate initial concentration, pH, temperature and contact time. The data obtained was fitted to kinetic and isotherm models to determine the mechanism. The adsorbent magnetite nanoparticles (Fe_3O_4) were synthesized by green synthesis using *Moringa olifera* and coprecipitation method. The characterization analyses of both green and chemically synthesized nanoparticles were performed by SEM, XRD, and FTIR. Both types of nanoparticles were found as magnetite (Fe_3O_4) with spherical shape. The average crystallite size of gINPs was 14.3 nm which conforms with the particle size determined from SEM Images. Batch adsorption experiments were conducted to study the adsorption kinetics and isotherm on gINPs, and samples were analyzed on High-Performance Liquid Chromatography (HPLC) at 280 nm. The results showed that 86.15% removal efficiency of levofloxacin was achieved using gINPs at optimal contact time i.e., 24 h when all other parameters were constant. Moreover, using different initial concentrations of levofloxacin, highest adsorption capacities obtained were 22.47 to 26.63 mg/g when the data fitted to Langmuir and Freundlich models, respectively. The pseudo-second order model described the adsorption kinetics data, fitting better than pseudo-first order with $R^2 = 0.965$, which means that the adsorption was chemisorption, exothermic and spontaneous. In addition, isotherm data obeyed Freundlich efficiently compared to the Langmuir isotherm with $R^2 = 0.994$ which means the adsorption was multilayer, and surface of adsorbent was heterogenous and non-uniform. The maximum adsorption capacity and removal efficiency were also achieved at pH 7 and 25°C for different levofloxacin concentrations. The potential pathway for levofloxacin' removal determined was chemisorption, spontaneous and exothermic onto the gINPs.

Chapter 1

Introduction

1.1. Background

Rapid globalization, industrialization and urbanization have led to advancement in human society and their associated environmental problems. Environmental problems which have attracted more attention worldwide in 21st century are water, soil and air pollution along with climate change (Yu *et al.*, 2016; Wu, 2017). But since last decade, major environmental concern is water pollution with emerging environmental contaminants due to their potential to cause detrimental effects on public health and ecosystem. Among these contaminants, pharmaceutical products and their residues got more attention as they are biologically active compounds with low biodegradability and mainly increased the waste treatment and disposal problem (Guo *et al.*, 2020). Pharmaceutical industries designed antibiotics for bacterial control in humans and animals. Antibiotics are extensively being used in aquaculture, agriculture and livestock industry as growth promoters and for clinical therapy (Tan et al., 2017). Consequently, antibiotics occurrence in water and wastewater widely reported in many countries. Antibiotics have various potential risks directly and indirectly. Directly the antibiotics have acute toxic effect on creatures and indirectly have most serious risk, which is potential, chronic antibacterial resistance. Antibacterial resistance means antibiotics gradually become ineffective against disease resistance (Deegan *et al.*, 2011). Manufacturing industries and wastewater are adding antibiotic residues from human, livestock, aquacultures and agriculture usage into environment (Da'na et al., 2018).

1.2. Consumption Pattern of Antibiotics

Tracking antibiotic consumption pattern over time give its trends and drivers. Antibiotics extensively used for human and animal health and as growth promoters for animals and plants (Dorival-García *et al.*, 2013). World Health Organization (WHO) reported that antibiotic global consumption rate from 2000 to 2015 rose by 65% and Defined Daily Doses (DDD) were 34.8 billion. Consumption rate in high income countries was lower than low and middle- income countries, however this data was based on only 76 countries and it included only those which humans consumes but not those which are consumed in animals for disease diagnosis, promoting growth, used for

growth of plants, excreted in municipal wastewater and residues in pharmaceutical wastewater (Klein *et al.*, 2018).

Pakistan has growing pharmaceutical industry. There are 759 manufacturing units including 25 multinational companies in Pakistan which fulfilled 80% need of county and 20% is covered by imports (pbs.gov.pk). There are 5000 registered drugs in Pakistan and growth volume is 17% per year. Pakistan local consumption off pharmaceuticals is US$1 billion (TRTA II Programme: Extended - TRTA Pakistan, 2020). The pharmaceutical industry imports almost 91% of all raw materials. The local raw material availability is restricted to followings: Amoxicillin, Ampicillin, Ciprofloxacin, Ofloxacin, Cephalexin, Cefradine, Cloxacillin, Ephedrine, Cephalexin, Cefradine, Cloxacillin, Ephedrine, Parabinez, Piperazine, Pyrazinamide, Cefixime, Cefadroxil, Cephalexin, Norfloxacillin, Santonin and Flucloxacillin. These raw materials do not meet the needs and major portion of standards is still imported (PPMA/Pharma Bureau-OCCI). Such large consumption and no legislation regarding their production, utilization and discharge led to substantial release of these compounds into environment.

1.3. Antibiotics Fate and Environmental Threat

Antibiotics enter the environment by numerous ways. The main sources of antibiotics contamination are pharmaceutical manufacturing plants, hospitals, wastewater treatment plants, aquacultures, agriculture, landfills, and private households. Municipal wastewater is the most common route of entry (Figure 1.1) (Arshad and Zafar, 2020; Mohapatra *et al.*, 2016). The dose given to humans and animals remains 30% to 90% un-degradable and excreted in active forms (Pouretedal and Sadegh, 2014). These antibiotics end up in soil and surface water (Yu *et al.*, 2016) by manure applications (Moraru *et al.*, 2012) as it contains high amount of nitrogen and phosphorus nutrients (Bolan *et al.*, 2010), reclaimed wastewater used for irrigation of agricultural land, (Kumar *et al.*, 2005; Gulkowska *et al.*, 2008), grazing animals and ultimately in surface water and then drinking water (Sim *et al.*, 2011).

Excessive release of antibiotics in environment poses serious threat which is not yet recognized by the world. Major threat is that antibiotics with time lose power on diseases as bacteria become resistant to them and it is difficult to overcome (Rehman *et al.*, 2015). From soil and use of reclaimed wastewater for agriculture, these antibiotics uptake by plants and may affect their physiology and growth (Leng *et al.*,

2020). Animals and birds do grazing on those plants and may be damaged as in past a drug Diclofenac sodium which have antimicrobial effect linked with renal failure of vultures and contributed more than 95% decline in its population in South Asia (Lonappan *et al.*, 2016; Fan *et al.*, 2020). From wastewater treatment plants, soil, agriculture, aquacultures, municipals and groundwater, it goes to surface water (Pina *et al.*, 2020) and used for various purposes like agriculture and drinking purpose where it can cause serious diseases in animals and humans like methemoglobinemia, dysbacteriosis and even kidney damage (Rodríguez *et al.*, 2020). It also disturbs aquatic ecosystem (Rodriguez-Mozaz *et al.*, 2015).

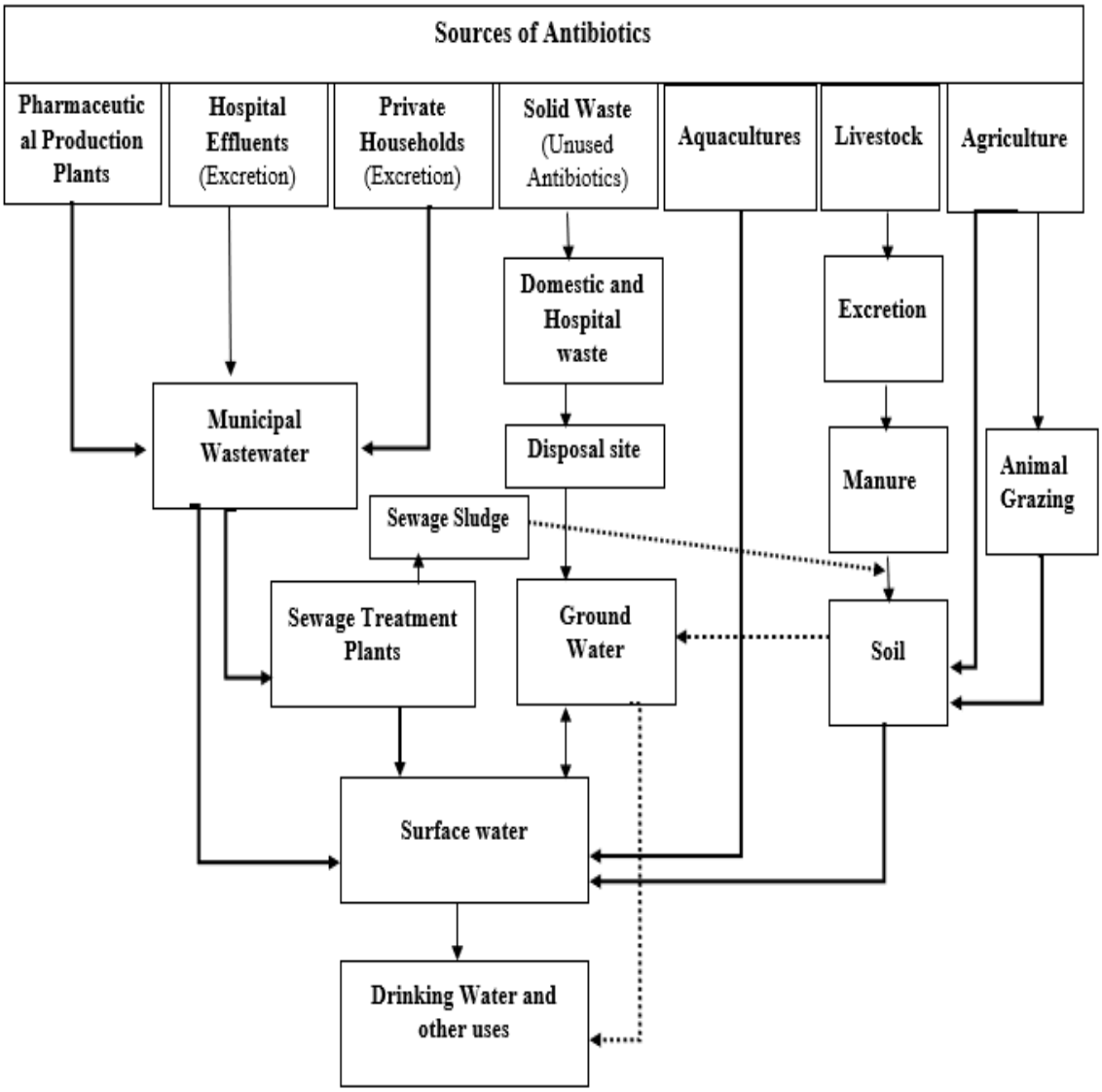

Figure 1.1. Occurrence and pathways of antibiotics in the environment

1.4. Antibiotics Removal

It is an emerging challenge for wastewater industry to remove antibiotics. Some recent scientific studies have been conducted and applied different treatment methods on antibiotic containing wastewater which ranges from biological to physical methods (Phoon *et al.*, 2020), single unit to combined system and adsorption to oxidation but currently, relevant data is very limited to generate common treatment method for antibiotic containing wastewater (Yan et al., 2017; Sabri *et al.*, 2020).

For antibiotics removal, adsorption is considered as the most fitted method because of availability of high range of adsorbents, high efficiency in less time and cost-effectiveness (El-Maraghy et al., 2020). As compared to other adsorbents magnetite nanoparticles has gained great attention in environmental remediation due to favorable properties for adsorption as it has high adsorption ability, easy preparation, enough stability, convenient operation, large surface area, facile recycling and biological sources (Ali *et al.*, 2020; Zhang *et al.*, 2020). Magnetite increases remediation efficiency as it carryout reactions on core and its shell at a time (Demirezen et., 2019). Magnetite can be made from various methods but green synthesis from plants, algae, fungi and bacteria can also be used for production of iron oxide nanoparticles. It is ecofriendly, energy efficient, low cost method and also reduces negative effect of chemical synthesis (Lin *et al.*, 2020; Weng et al., 2020; Wu *et al.*, 2020). *Moringa olifera* is the major crop of Africa and Asia and belongs to family Moringaacea. *Moringa olifera* leaves have high content of carbohydrates, polyphenols, flavonoids, tannins and antioxidant compounds (Sreelatha and Padma, 2009; Saini et al., 2016).

The goal of the current study was to synthesize iron oxide nanoparticles and testing its ability and efficiency to remove levofloxacin antibiotic from wastewater.

1.5. Objectives of the Study

The main objectives of the present study were:

i. Green synthesis of iron oxide (Fe_3O_4) nanoparticles and their characterization
ii. Potential of green synthesized Fe_3O_4 nanoparticles for removal of selected antibiotic from wastewater.
iii. Understanding the primary mechanism of antibiotics removal.

1.6. Scope of Study

Antibiotics are being used in large quantities for humans, animals, agriculture, and aquaculture worldwide. Antibiotics in water promote spread of resistance in bacteria,

pose significant risk to human health and disturb ecosystems upon entry into food chain. The antibiotics in water may kill beneficial bacteria in surface and subsurface water. Therefore, scope of this study was to develop antibiotics' removal method for antibiotics-bearing wastewater.

Chapter 2

Review of Literature

2.1. Emerging Environmental Contaminants

Emerging contaminants (ECs) are referred as group of pollutants which are highly toxic even at low concentration. These contaminants because of their peculiar behavior have gained more attention all over the world (Cheng et al., 2021). These are predominantly unregulated chemicals mostly contributed by anthropogenic sources and become part of water, air, soil, food. Emerging compounds are not easy to degrade because of their high persistence in environment. They have long retention time. Important types of ECs range from pharmaceuticals, surfactants, plasticizers, pesticides, and personal care products (Rout et al., 2021).

2.2. Pharmaceutical compounds

Pharmaceutical compounds have controlled production and utilization. There is no proper mechanism available for the disposal of these compounds. Antibiotics are considered as one of the important class of pharmaceutical compounds because of different characteristics including partial metabolism, persistent nature, and easy translocation (Pathak et al., 2020).

2.3. Antibiotics

Antibiotics are used to eliminate or degrade the progress of microbes. These are derived from the bacterium with high resistance against the microorganisms as special secondary metabolites. Several classes of antibiotics exist like Fluoroquinolones, β-lactams, Sulfonamides, and Tetracyclines, etc. (Walsh, 2003). Fluroquinolones are widely used in Pakistan and removal of one of the antibiotics of this class has been studied. These antibiotics are used against the infection induced by *E. coli, Salmonella* and *Campylobacter*. Fluroquinolones are used in various industries including agriculture, aquaculture, medicine and poultry. Ofloxacin and levofloxacin are some common examples of Fluroquinolones. Since 2005, production and export of Fluroquinolones for the sake of poultry related uses is prohibited in Australia, America, Denmark and Sweden (WHO, 2013). Figure 2.1 describes the general structure of Fluoroquinolones. Aromatic ring, hydroxyl group and carbonyl group replace the R1 and R2 present in the structure of Fluroquinolones. Levofloxacin is an isomer of ofloxacin (Mouzam et al., 2011). Levofloxacin can be used effectively for the treatment

of both Gram positive and Gram-negative bacteria. Levofloxacin is from the third generation of fluoroquinolones.

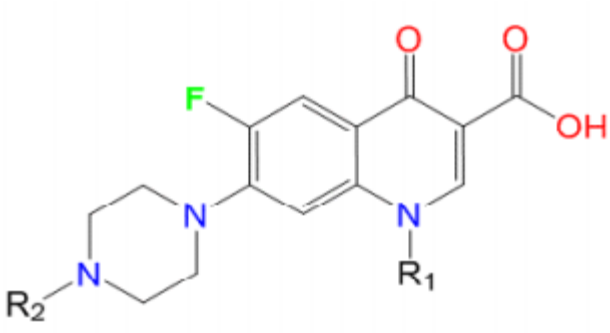

Levofloxacin:
R_1 = aromatic ring with carbonyl group,
R_2 = Hydroxy group

Figure 2.1. General Structure of Fluoroquinolones

2.4. Antibiotics as pollutant in Environment

Antibiotics are used at broader spectrum so there are various potential sources which may introduce antibiotics into the environment. These sectors are hospitals, agriculture, livestock and aquaculture, pharmaceutical plants, and animals' farms. Antibiotics display various pathways and translocation patterns to enter the environment. They become part of groundwater and freshwater. Ultimately this waster is used for drinking and irrigation purposes as shown in Figure 1.1 (Arshad and Zafar, 2020). Activated sludge is used as a wastewater treatment process but it cannot be used for the removal of antibiotics because of its low efficiency for antibiotics removal. Antibiotics cannot break down in bodies of humans and animals. Discharge of antibiotics into the ecosystem is the ultimate fate and emerging environmental problem of time as well (Gao et al., 2015). Different types of wastewaters contaminated with antibiotics are mentioned in below.

2.4.1. Pharmaceutical industry wastewater

Wastewater with excessive number of organic materials and antibiotics compounds and other toxic compounds is stated as pharmaceutical wastewater. Approximately 1 ton of antibiotic residues generate antibiotic wastewater within the range of 150-200 m^3 (Ji et al., 2013). China is one of the bigger consumers and producers of antibiotics at the same time. In 2009, annual export of antibiotics was around 2.5 million whereas production was worth of 14.7 million. For the same year, global production of antibiotics was 20 million (Guo et al., 2012). Yang et al. (1997) stated that accumulation and distribution of antibiotics in water cycle is because of manufacturing processes. Strong color, smell

and large variation in both quality and quantity of wastewater occur. Antibiotics lower the pH of wastewater. Other attributes of manufactured wastewater include high suspended solids and high COD level i.e., 500-25,000 and 10,000-80,000 mg/L, respectively. More detail is given in the table 2.1.

Table 2.1. Pharmaceutical industry wastewater characteristics (unit: mg/L)

Antibiotic	Production Process	COD	Antibiotic Residue
Tetracycline	Extraction	20,000	1500
Oxyletracycoine	Crystallization	10,000-35,000	1000
Lincomycin	Solvent recovery	15,000-20,000	50-100
Ofloxacin	-	-	110
Kanamycin	Extraction	25,000-30,000	80
Ampicillin	Solvent Recovery	5000-70,000	0.54 % (Open ring)

(Brown et al., 2006; Yang et al., 1997)

India has a significant role in the production of antibiotics all over the world, as an important antibiotic's producer. High concentration of ciprofloxacin i.e., 31 mg/L was found in the effluents of drug manufacturer industry in India (Fick et al., 2009).

2.4.2. Wastewater Treatment Plants (WWTPs)

Antibiotics released from the hospital wastewater and manufacturing units are diluted when mixed with municipal waste. High concentration of ciprofloxacin i.e., 14 mg/ L emitting from a drug manufacturer plant in India has been found (Fick et al., 2009). Table 2.2 shows the antibiotics residues identified in wastewater treatment plants.

Table 2.2. Antibiotics reported in WWTPs

Antibiotic	Concentration (µg/L)	Reference
Sulfamethoxazole	0.39,0.31, 1, 1.25,2.8	(Brown et al., 2006; Batt et al., 2007)
Ofloxacin	0.47,0.11,0.40,1,0.165	(Brown et al., 2006; Xu et al., 2007)
Levofloxacin	0.301	(Yasojima et al., 2006)
Ciprofloxacin	0.20, 1, 45.0	(Brown et al., 2006; Sim et al., 2010)
Trimethoprim	72.85, 0.813	(Segura et al., 2015; Peng et al., 2014)
Tetracycline	1.2	(Karthikeyan and Meyer., 2006)

2.4.3. Hospital wastewater

Antibiotics from the hospital wastewater are also accumulated into the environment. According to a report presented by Dinh et al. (2017), concentration of residual antibiotics in the hospital effluents (coming from the hospital) is 3-10 times greater compared to the antibiotics present in freshwater and wastewater treatment plants. It was assumed that antibiotics present in wastewater have not been mixed with another environment. Hospital wastewater was a raw effluent. Higher amount of SMX of 28.36 µg L^{-1} have been found by Lee et al. (2016) in hospital wastewater. Table 2.3. demonstrated the different antibiotics reported in the hospital wastewater.

Table 2.3. Antibiotics reported in hospital wastewater

Antibiotic	Concentration (µg/L)	Reference
Sulfamethoxazole	0.8,2.1,0.4, 28.36	(Brown et al., 2006; Lee et al., 2016)
Ampicillin	0.2-80	(Kimosop et al., 2016)
Azithromycin	4.9	(Aydin et al., 2019)

Ciprofloxacin	0.20, 1, 45.0	(Brown et al., 2006; Sim et al., 2010)
Trimethoprim	6.65	(Brenner et al., 2010; Peng et al., 2014)
Tetracycline	6-53.17	(Lien et al., 2016)

2.4.4. Surface water

The antibiotics occurrence in the surface water has been widely reported. Table 2.4 shows the occurrence of antibiotics in different kinds of surface waters around the world.

Table 2.4. Antibiotics reported in surface water

Antibiotic	Concentration (µg/L)	Reference
Sulfamethoxazole	23.35	(Koreje et al., 2012)
Erythromycin	1.6	(Yao et al., 2017)
Enalapril	1.5	(Fick et al., 2019)
Trimethoprim	13.68	(Zhang et al., 2012)

Concentration of antibiotics is comparatively high in the proximity of their application including animal farms and hospitals. Distribution of antibiotics in freshwater bodies and surface water, spatially and temporally is needed to be investigated yet.

2.5. Scenario of pharmaceutical industry and antibiotic pollution in Pakistan

Annual increase in growth rate of pharmaceutical industry of Pakistan ranges from 10%-20% comprising of US$ 4.0 billion approximately. More than 750 pharmaceutical formulation units are working in Pakistan now. Different 25 multinational companies are also working in Pakistan. Pakistan pharmaceutical industry contributes an export of 300 million US dollars whereas local industry has the potential to meet 98% demand of medicine in the form of finished products. Following table displays the concentration of antibiotics reported in the streams of Pakistan.

Table 2.5. Antibiotics detected in wastewater streams of Pakistan (Zafar et al., 2021 & Khan et al., 2013)

Antibiotic	Conc. *(*mg L^{-1}*)*
Erythromycin	0.0011
Lincomycin	0.0041
Ciprofloxacin	332.154
Ofloxacin	2.558
Levofloxacin	6.63
Oxytetracycline	0.027
Trimethoprim	0.028
Sulfamethoxazole	16.009
Ampicillin	32.57

It evident from the various studies performed in Pakistan that antibiotics are present in different media at various concentrations. In Pakistan poultry meat contained different antibiotics namely, amoxicillin, quinolones, and tetracycline, with concentration of 16.92-152.62, 20-30.81 and 89.2-800 µg kg^{-1}, respectively. A study by Khan et al. (2018) projected that antibiotics are presents in almost 38% of 300 raw samples of beef. A study was performed for the analysis of milk samples in Sindh, Pakistan. Results concluded that 36% samples were confirmed with the presence of beta-lactams whereas 56% portion of milk was contaminated with amoxicillin and 48% with ampicillin (Khan et al., 2018).

2.6. Impacts of antibiotics

Antibiotics have various ways to enter the environment and concentration of antibiotics vary in different compartment of the environment. Impact of antibiotics on the human and environmental health is discussed below.

- Antibiotics cause stress on water resources by exploiting and degrading the water quality.
- Sludge is rich in the organic contents and antibiotics piled up in the sludge and use as fertilizer to enhance the productivity of crops (Lamastra et., 2018).
- Antibiotics can potentially harm the life of aquatic animals i.e., excess amount of antibiotics present in water can kill them. Fish embryo can be harmed till death within 24 hours by antibiotics in development phases. These aquatic animals when become part of food chain can cause biomagnification and bioaccumulation of toxic substances. Contamination of antibiotics in the aquatic environment can limit the algal growth (Bielen et al., 2017).
- More than 50% population of world is dependent on the agriculture as their source of livelihood. Antibiotics can induce negative impact on the agriculture. It can inhibit the potential growth of crops and plants. It does not only degrade the quality of food but also reduce the quantity of food. Twenty million hectares of land is irrigated with wastewater which comprises 10% of food production linked to the one billion people associated with it (Blaire and Laura., 2018).
- Introduction of antibiotics into the environment can alter the microbial community and enhance the resistance in the bacteria. Increase in the resistance ability of bacteria can directly increase the death rate. It increases the potential of health sickness and reduce the effectiveness. Bacteria with more resistance are not easy to treat which ultimately expand the survival threat for humans. Healthcare cost also upsurges for the treatment (Bielen et al., 2017; UN Report., 2014).

2.6. Treatment technologies for antibiotics removal

Owing to the diversity in physical, chemical and biological attributes of antibiotics, it is very difficult to remove them from the aquatic ecosystem. There is no treatment technology found for the complete removal of antibiotics yet. However, antibiotic-containing wastewater passes through the mechanical, chemical, and biological processes in a wastewater treatment plant. Traditional sewage treatment plants are not useful for the removal of antibiotic-containing wastewater. Amount of antibiotics entered the treatment plant is very high compared to the amount remove by the conventional treatment plants (Van Dorslaer et al., 2014). Treatment of antibiotics is also difficult to perform because of antimicrobial properties and

structure of antibiotics. Three types of treatments used for wastewater and water including physical, chemical, and biological. Table 2.4 is about the characteristics, advantages, and limitations of biological, physical and chemical treatment methods.

Table 2.6. Antibiotics Treatment methods and their limitations

Treatment	Characteristics	Advantages	Constraints
Physical Methods			
1. RO (Wang et al., 2018)	Membrane technology to force a liquid by pressure	▪ Multibarrier approach ▪ High quality effluent	Only retains contaminants and cause breeching of membrane
2. Microfiltration/ Nanofiltration (Wang et al., 2018)	Filtration	Suitable for limited space & high-quality effluent	▪ Unsuccessful for AB removal ▪ Expensive and energy intensive
3. AC (Granzota et al., 2021)	Filters and adsorbs material applied as granular or powdered feed	GAC: steam method increased the adsorption and easily recovered	▪ Proper for clean water ▪ Fed continually
Biological Methods			
1. MBR (Wang et.al., 2018)	Combine membrane technology with AS	Suitable for limited space	Pollutants accumulated in brine
2. SBR (Frenandez et al., 2009)	AS two or more tanks work in sequence	Process can be modified easily	Shock loads effect stability
3. AS (Lofrano et al., 2017)	▪ Handled a lot of organic waste. ▪ Microbial digestion with aeration	▪ Extensively applied. ▪ Cost-effective	Shock loads effect stability

4. BFR (Grandclement et al., 2017)	Material is supported by microbes	Less down time and stable operation	Cells build up and causes blockage
5. UASBR (Arias et al., 2018)	Anaerobic stage reactor with separate methanogenesis & acetogenesis	Less sensitive to shock loads and variables, No mixing	Antibiotics may kill or causes resistance in bacteria
Chemical Methods			
1. O_3 (Homem and Santos., 2011)	O_3 addition and oxidation	Allows ABs mineralization but good disinfectant	Expensive and energy demanding
2. Chlorination (Matamoros and Salvado., 2013)	Chlorine addition used for drinking water	Good disinfectant	By-products' formation which is linked with cancer
3. Flocculation (Matamoros and Salvado., 2013)	Coagulants and flocculants added for settling of pollutants	May settle small size pollutants like hormones	Expensive and not enough efficient for antibiotics
4. Per-ozonation (Homem and Santos., 2011)	Mixture of H_2O_2 and O_3 for oxidation	More efficient than ozonation	Expensive and energy demanding
5. TiO_2 (Xing et al., 2018)	Super oxide radical and hydroxyl generation to react with pollutants	For removal fixed to film or beads	Expensive and energy demanding
6. Photolysis (Xing et al., 2018)	Light absorption to directly breakdown compound	Inexpensive	For sunlight, dependent on geographical area
7. Photo-Fenton (Granzota et al., 2021)	OH-generation and coupled with UV	Iron is non-toxic and plentiful	Energy demanding and iron sludge disposal

From the above table, it can be concluded that each treatment method has some limitations like low efficiency, high cost and energy demanding, etc. and there is need of treatment method which should be cost-effective, efficient, less energy demanding and environment friendly. Method used in this study is of adsorption by iron oxide nanoparticles.

2.8. Iron oxide (Fe_3O_4) nanoparticles and adsorption mechanism

Magnetite nanoparticles work as reductant and adsorbent for removal of antibiotics as the structure of iron oxide nanoparticles consists of two parts namely iron core and oxide shell. The removal of antibiotics on iron oxide done by adsorption, precipitation on oxide shell and by reduction on iron core. The structure of iron oxide nanoparticles is shown in figure 2.2 (Li et al., 2014; Saif et al., 2016).

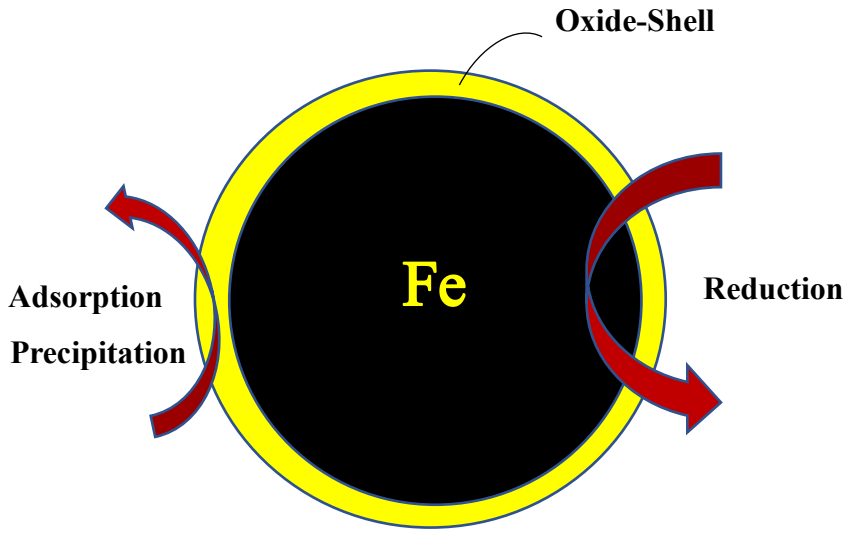

Figure 2.2. Structure of Iron oxide nanoparticles and AB removal processes

Adsorption is the process of separation of specific compound between the solid phase of adsorbent and liquid phase of adsorbate. For removal of different contaminants, adsorption has been applied in previous studies. The maximum efficiency of adsorption by specific adsorbate can be determined by changing the adsorbate properties like Concentration of adsorbate, pH of adsorbate solution, temperature on which experiment would be conducted, pressure and reaction time (Sun et al., 2015; Kovalova et al.,

2013). The mechanism of adsorption mainly involves steric mechanism, equilibrium mechanism, and kinetic mechanism.

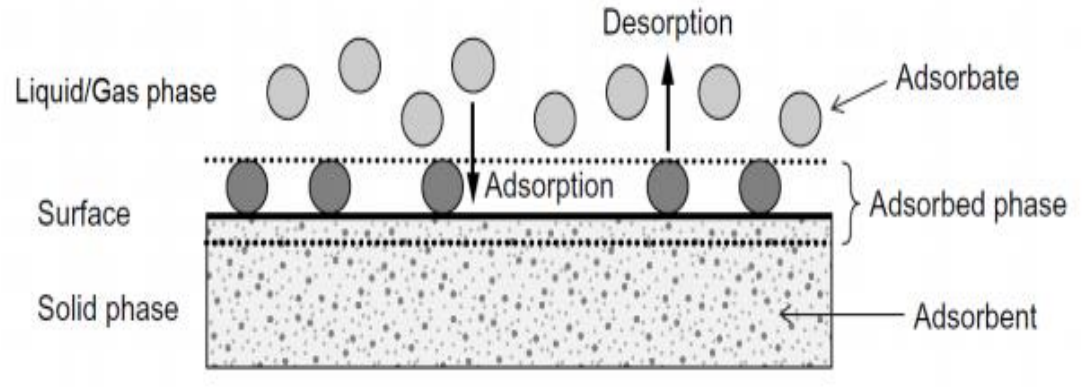

Figure 2.3. Adsorption Elements (Worch, 2012)

Steric mechanism based on the pores of adsorbent as small molecules enter easily but large molecules are not allowed by pores. Equilibrium mechanism depends upon the affinity of adsorbate and adsorbent. As adsorbent can be applied to different adsorbates, the one which have high affinity adsorbed more by the adsorbent and reaches its equilibrium point. Kinetic mechanism depends on the bond breakage of adsorbate compound and chemical affinity with adsorbent to form bonds. Kinetic mechanism also depends on the rate of diffusion of adsorbate into adsorbent pores. Adsorption process can be controlled by the time of reaction between adsorbent and adsorbate (DO, 1998; Loulidi et al., 2020). Therefore, selection of adsorbent matters a lot for removal of pollutants. The mechanism of adsorption is shown in Figure 2.3 (Worch, 2012).

2.9. Nanoparticles' preparation methods

There are various methods for the preparation of nanoparticles but in this study, it was conducted by two methods namely green synthesis and coprecipitation, a chemical method.

2.9.1. Green Synthesis

Nanoparticles can be synthesized biologically from plant materials like leaves, pericarp, seed and fruit, fungi, microbes, and algae. These biologically synthesized nanoparticles are more preferred as they are cheap, environment friendly, safe, and easy to scale up. Biologically synthesized nanoparticles are being used in different fields for different

purposes (Rana et al., 2020). Biological synthesis of nanoparticles using plant extract was firstly reported by Gardea-Torresdey et al. (2003). They prepared silver nanoparticles from *Alfalfa sprouts.* In green synthesis, the plant biomaterial like flavonoids, polyphenols, hydroxyl, carboxylic group and terpenoids when react with metal ions form nanoparticles by acting as capping, reducing, and stabilizing agents (Demirezen et al., 2019; Saleem and Fouda, 2020). The possible reaction that occurs is given below.

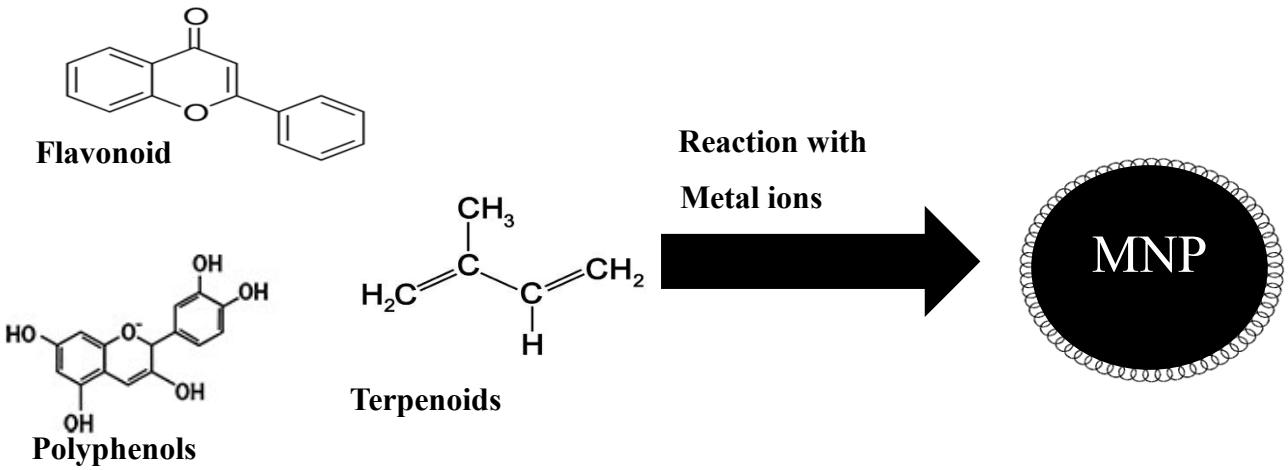

Figure 2.4. Role of plant biomaterial in green synthesis

Moringa olifera leaves can be used for green synthesis of magnetite nanoparticles as Vongask et al. (2013) reported that 100 g of M*oringa olifera* leaf extract contained 13.23g of phenolics and 6.20 g phenolics which means that it has good ferric reducing power (51.50 mmol $FeCl_3$). It is commonly known as "Drumstick or Horseradish Tree and "Sohanjna or Sahajna." The scientific classification of *Moringa olifera* is shown in table 2.7.

Table 2.7. Scientific classification of *Moringa olifera*

Scientific Classification	
Kingdom	Plantae
Class	Tracheophyte
Order	Brassicales
Family	Moringaceae
Genus	Moringa

Species	olifera

It was selected on the basis of following properties.

- Its abundance as it is native to tropical Asia but also adapted in Africa and tropical America.
- Indigenous to Pakistan as it is common all over the plains of Punjab, in the foothills of Himalayas, and other foothill ranges in the north and west.
- Fast growing and perennial
- Used for different purposes (Orwa et al., 2009).

2.9.2. Coprecipitation Method

It is simple, facile, classical, and convenient method of nanoparticles synthesis. It is extensively applied for industrial and research objectives due to its easy operation. In this method, precipitation of soluble compounds is conducted for nanoparticles' synthesis. In case of magnetite synthesis, Fe^{3+} and Fe^{2+} ions give the following reaction in oxygen free environment (Nawaz et al., 2019).

$$Fe^{2+} + 3Fe^{3+} + 8OH^{-} \rightarrow Fe_3O_4 + 4H_2O \qquad \text{(Equation 2.1.)}$$

So, coprecipitation method can be used for nanoparticles synthesis but it is totally dependent on chemicals, not environment friendly, expensive, and toxic.

Just to summarize this part of thesis, there are serious concerns about the release of antibiotics into the environment. Current treatment methods for wastewater are not capable of removing antibiotics fully. Presence of these pollutants is harmful for the environment and human health. There is need to develop innovative methods to address the problem and control the dissemination antibiotics in the environment.

Chapter 3

Materials and Methods

The aim of this study was to develop a method for removal of antibiotics (levofloxacin) from wastewater/ aqueous solution with the help of iron oxide nanoparticles prepared by green synthesis. Even though the concentration of antibiotics detected in environment within range of µg L^{-1} and ng L^{-1} but their continuous release into environment and persistent nature makes them pseudo-persistent pollutants. Chemical synthesis of iron oxide nanoparticles was conducted to confirm the green synthesized nanoparticles formation and efficiency of green synthesized iron oxide nanoparticles was evaluated for levofloxacin removal. The tree of research methodology is presented in Figure 3.1.

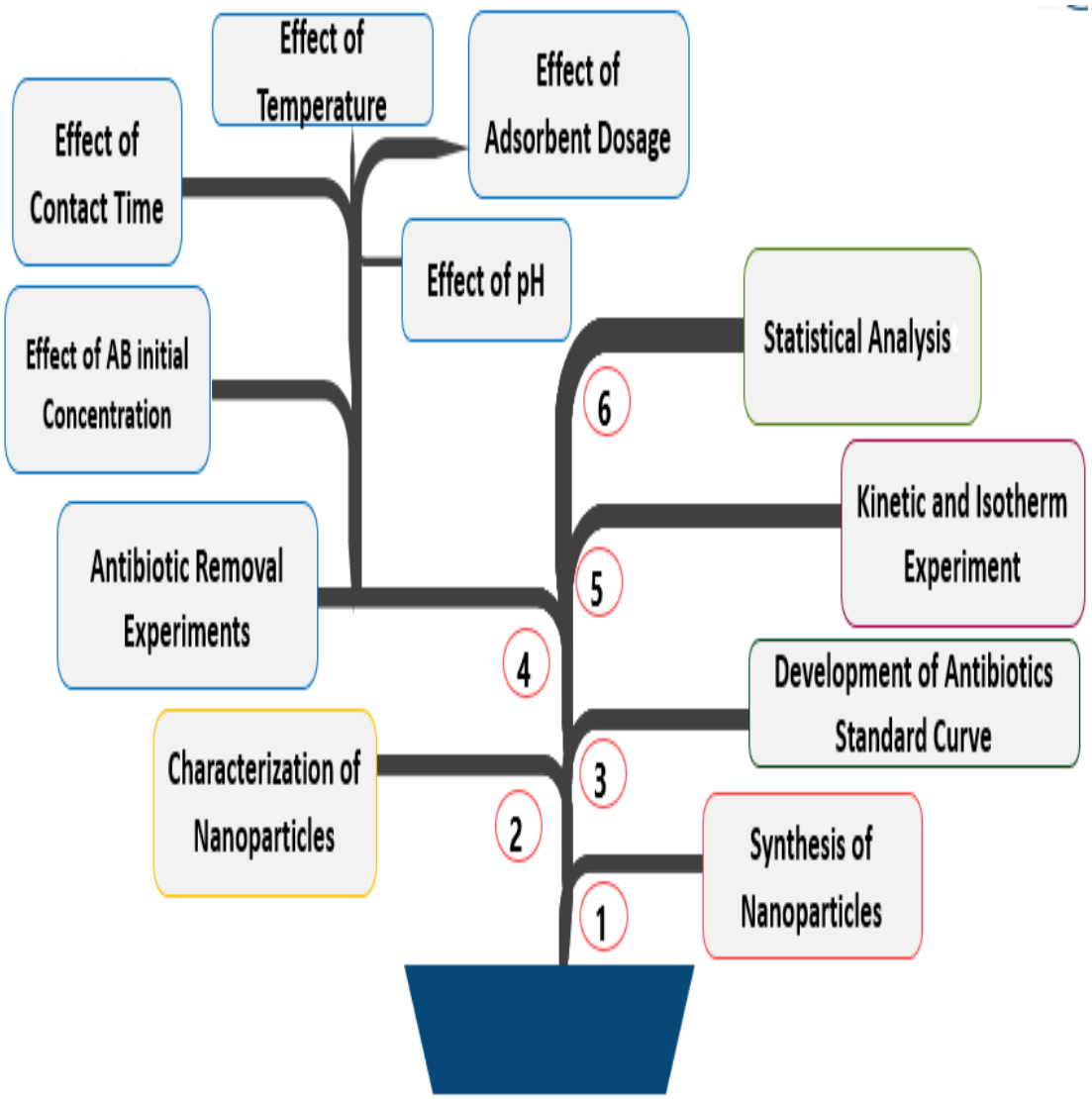

Figure 3.1. Research methodology tree

3.1. Materials and Reagents

Pure salt of levofloxacin (Levo) was procured from Sigma Aldrich, Germany through local vendor. Levofloxacin was selected to represent the Fluoroquinolones, one of the most commonly prescribed and reported class of antibiotics in wastewater samples. Its chances of release into environment are high due to its high demand and consumption pattern. All the chemicals namely ferrous chloride, ferric chloride and NaOH used in preparation of nanoparticles were of analytical grade. All the chemicals and reagents used in antibiotic analysis on HPLC were of HPLC grade. Distilled water for nanoparticles preparation and experimental use was obtained from distillation unit available within the laboratory. Syringe filters with pore size 0.25 µm and, disposable but sterilized syringes of 3 mL range were used for sample and nanoparticles separation where required.

3.2. Nanoparticles Synthesis

Iron oxide nanoparticles were prepared by two techniques namely Green Synthesis method (using plant leaves) and Coprecipitation method.

3.2.1. Green Synthesis

a) Plant leaves collection and extract preparation

Moringa olifera plant was selected based on its abundance in Asia and its leaves' chemical composition possesses high content of polyphenols and flavonoids. *Moringa olifera* plant fresh leaves were collected from Vehari District of Punjab. First, leaves were rinsed with distilled water and air-dried in sunlight. For preparing the leaves extract, vegetal material (leaves) and distilled water was adjusted in 20:100 (weight/volume), respectively. The fresh and finely sliced *Moringa* leaves were boiled for 20 minutes at 70-80°C and 700 rpm on hot plate stirrer. Extract was filtered under normal gravity using Whatman No.1 filter paper. Then final volume of extract was raised to 100 mL by washing the leaves residue with distilled water and stored for one week (Stan et al., 2017).

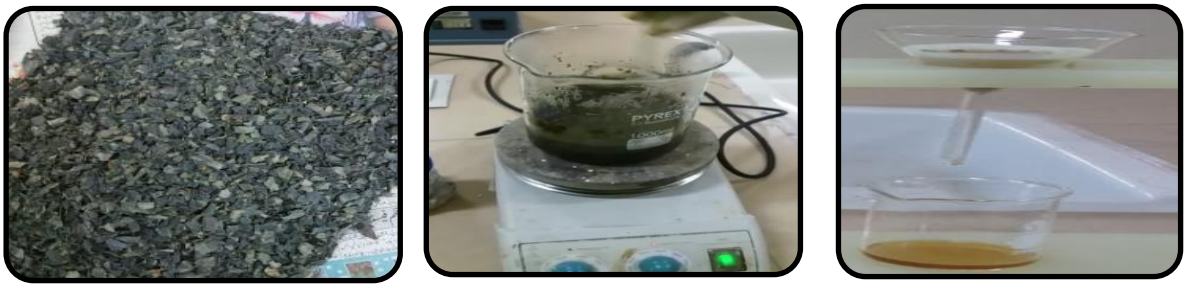

Figure 3.2. Different stages of preparation of *Moringa olifera* leaf extract

b) Synthesis of iron oxide nanoparticles (gINPs)

For synthesis of gINPs, ferrous and ferric salts of iron were mixed with 1:2, respectively. Precisely, 5.3 g of ferric chloride ($FeCl_3.6H_2O$) and 2.65 g of ferrous chloride ($FeCl_2.4H_2O$) were dissolved in 500 mL distilled water at 80°C under mild magnetic stirring on hot plate stirrer. After 30 mins, they were dissolved completely, and light orange color appeared as shown in Figure 3.3. Then, 25 mL of moringa leaf extract was added after 30 mins while stirring on hot plate. Solution turned brownish black from orange and after 5 mins, 100 mL of 1M NaOH was added, and black precipitates of magnetite (Fe_3O_4) were formed as shown in Figure 3.3. Further, after 5 minutes of stirring, solution was removed from hot plate and left for settling down of iron oxide nanoparticles precipitates. Black precipitates were washed five to eight times and oven dried at 80°C for 8 hours (Demirezen et al., 2019; Stan et al., 2017). Then, the precipitates were crushed by pestle and mortal and stored in tightly closed glass jar. Magnetite yield by this method was 4.5 g per batch.

Figure 3.3. Different step in synthesis of gINPs

3.2.2. Chemical Synthesis (Co-precipitation Method)

Chemical synthesis of magnetite was conducted by co-precipitation method. One molar solution of ferric chloride ($FeCl_3.6H_2O$) and ferrous chloride ($FeCl_2.4H_2O$) were prepared by adding 19.8 g and 27.03 g in 100 mL distilled water of both, respectively. Then 0.1 M solutions were prepared from 1 M solution. Further process was carried on hot plate stirrer. Nitrogen gas was purged in 700 mL distilled water in 1000 mL beaker at 25°C and stirring at 200 rpm. After 2 minutes of nitrogen purging, 50, 100 and 70 mL of 0.1 M ferrous, ferric and 1 M NaOH solution were added, respectively, in

presence of nitrogen and stirring till 3 minutes. Solution turned black and precipitates were formed when NaOH was added. Black precipitates were washed five to eight times with distilled water. While washing, it turned into two layers as particles settled down making a layer and other layer was of water which was added for washing. The purpose of washing was to remove the NaOH which was added to make precipitates. The liquid was removed after each washing and 700 mL additional distilled water was added for subsequent washing and particles were oven dried at 80°C for 24 hours in hot air oven (Yazdaani and Seddigh., 2018). Magnetite yield by this method was 0.8 g per batch. After 24 hours of drying particles were crushed and converted into powder form, followed by storage in glass jar for further processing.

Figure 3.4. Chemically synthesized nanoparticles

3.3. Characterization of magnetite Nanoparticles

Magnetite nanoparticles were characterized by three methods: morphological structure was determined by Scanning Electron Microscopy (SEM), crystallinity and phase purity by X-Ray Diffraction (XRD) and presence of different functional groups by Fourier Transform Infrared Spectroscopy (FTIR). The specifications of sample preparations before each characterization and measurements are given below:

3.3.1. Morphological Structure

The morphological composition of both green and chemically synthesized nanoparticles was examined by scanning electron microscope (JSM-6490A, JEOL) with accelerating voltage of 10 kV. Sample was prepared by sonication of nanoparticles for 30 mins and particles were placed on slide with the help of needle. Before analyzing on SEM sample was sputter coated with gold to make it good conductor.

3.3.2. X-ray diffraction (XRD)

Diffraction pattern of prepared magnetite's was obtained by X-ray diffraction analysis (XRD, D 8 Advance Bruker diffractometer) with wavelength 0.15406 nm of Cu- Kα radiation (40 mA, 40 KV). Sample analyzed was in powder form. The parameters for XRD analysis were: 2-Theta range = 20-80°, Step size = 0.020°, Divergence slit = 0.5° and Time/step = 0.2s. The crystallite phase purity was assessed and through its pattern, crystallite size was calculated using Scherer equation (Equation 1). The XRD data was manipulated by Match software and Origin Lab.

$$L = \frac{k\lambda}{\beta cos\theta} \qquad \textbf{(Equation 1)}$$

Where:

L = Average crystallite size (nm)

K = 0.891 is crystallite shape factor

λ = 0.15406 is wavelength of X-ray (nm)

β = Full Width Half Maximum (FWHM) (radians)

θ = Diffraction angle

3.3.3. Fourier transform infrared spectroscopy (FTIR)

Fourier-transform infrared spectroscopy (FTIR) spectra of prepared samples were obtained by an infrared spectrum optical instrument - JASCO 6100 FTIR spectrometer. The technique used for sample preparation was KBr method (KBr disc) and measured at 4000 to 400 cm^{-1} scale range. The nanoparticles sample analyzed was in solid form, sample pellets were prepared by blending the sample with potassium bromide (KBr) with 1:200 (w/w) ratio, respectively. The total scans in scanned sample were 32 cm^{-1} and ranged 4 cm^{-1}. The FTIR spectra of both green and chemically synthesized nanoparticles was combined using origin Lab.

3.4. HPLC Protocol and Development of standard curve

Antibiotic (levofloxacin) analysis was performed by Agilent 1260 Infinity II LC system (High Performance Liquid Chromatography HPLC). It is equipped with auto sampler for auto injection, diode array detector and quaternary pump. Chromatographic separation was carried out with Eclipse (4.6 × 250 mm) C18, 5 µm analytical column. Mobile phase used was of acetonitrile and 1% formic acid with the ratio of 16:84,

respectively (Zafar et al., 2021). The measured pH of mobile phase was 4.9. The prepared mobile phase was sonicated for 30 mins at ambient temperature and then sterilized cellulose nitrate filter paper of 0.45 µm was used to filter it. For sample analysis, HPLC optimum conditions were as follow: 20 µL of antibiotic sample was injected via HPLC column with 1 mL per min flow rate. Column temperature was set to "not controlled" and it was around 35°C. Compound in sample was detected at 280 nm using DAD detector. Column washing using methanol and procedural blanks was performed on regular basis.

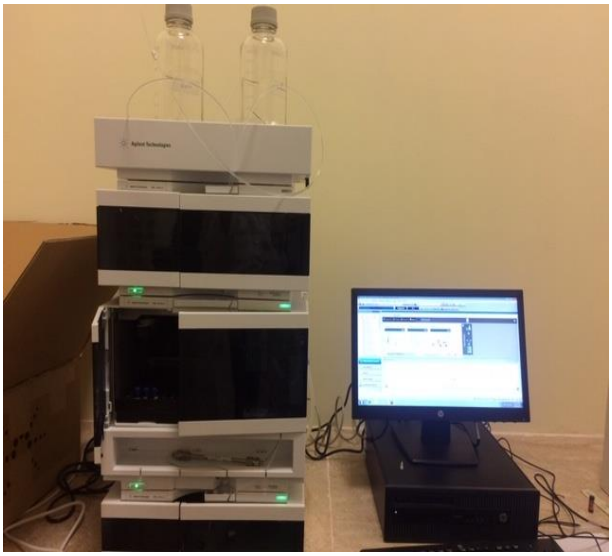

Figure 3.5. HPLC (Agilent 1260 Infinity II LC System)

For development of standard curve of levofloxacin, four standards of different concentration (10, 20, 30 and 40 mg/L) were prepared. All concentrations were analyzed at least for three time on HPLC to verify stability of retention time, peak area, as well as system. The single sharp peak of levofloxacin in chromatogram attributed to the purity of antibiotic. In case of levofloxacin, the retention time was 7.22 and sample run time was 10 min. Calibration curve was generated via plotting the peak area against concentration. Experimental samples were analyzed in duplicate, and their concentration was calculated using the trendline equation obtained from calibration curve.

3.5. Adsorption Batch Experiments

Antibiotic (levofloxacin) removal potential of iron oxide nanoparticles (gINPs) was assessed through batch experimental technique. Batch experiments were performed to reveal the effect of magnetite dosage, solution initial concentration, pH, temperature, and reaction time. Adsorption mechanism was determined by conducting Kinetic and Isotherm experiments. The detail methodology of independent experiment is given below.

3.5.1. Effect of magnetite dosage

Levofloxacin solution of 4 mg/L concentration having pH 6.45 (original solution pH) was prepared in distilled water. In order to find the optimum dose, five different adsorbent doses 0.005, 0.025, 0.050, 0.075 and 0.10 g L^{-1} were selected on the basis of literature. Each dose was added in different conical flasks containing 80 mL solution of 4 mg/L concentration. The flasks were placed in shaking incubator (LSI- 3016R, Korea) for 24 hours to ensure that equilibrium was attained, at 25 °C temperature and 150 rpm. After 24 hours 20 mL sample was collected with the help of syringe and nanoparticles were separated by external magnetic field, then passed through 0.25 µm syringe filter before injecting in HPLC vial for analysis and storage. For sample antibiotic (levofloxacin) concentration peak area obtained was calculated by using trendline equation obtained from standard curve. The removal efficiency and adsorption capacity were calculated for each sample.

3.5.2. Effect of adsorbate initial concentration

Five different initial concentrations of adsorbate were used to determine their effect on levofloxacin removal. Precisely, 4, 8, 12, 16 and 24 mg/L concentrations were prepared in distilled water. The adsorbent dose applied was the optimum dose (0.1 g/L) obtained from the dosage experiment. The experiment was conducted for 24 hrs in shaking incubator at 150 rpm and 25 °C. Sample was collected after 24 hrs, separated from nanoparticles, and passed through syringe filters before analyzing on HPLC.

3.5.3. Effect of solution initial pH

Solution initial pH effect was revealed by applying seven different pH of levofloxacin solutions. Solution pH was varied from 4 to 10 and different pH was adjusted with 0.1 M HCl and 0.1 M NaOH solutions. The pH was measured by multimeter (WA-2015) Taiwan. The adsorbent dosage and antibiotic (levofloxacin) initial concentration

applied was optimal. Experiment was conducted for 24 hrs in shaking incubator at 150 rpm and 25 °C. After 24 hrs, sample was collected, separated and analyzed.

3.5.4. Effect of Temperature

To determine the temperature effect four different temperatures 20, 25, 30 and 35 °C were selected whereas antibiotic (levofloxacin) initial concentration was 4 mg/L and adsorbent dosage applied was optimum. pH of the solution was maintained at which maximum removal efficiency was achieved. The experiment was conducted for 24 hrs at shaking speed of 150 rpm. Sample was collected after 24 hrs, separated, and analyzed.

3.5.5. Effect of contact time

To determine the reaction time effect, experiment was conducted for 24 hrs but sample was collected at time interval of 5, 10, 20, 40, 60, 120, 240 and 1440 mins.

The concentration of levofloxacin, adsorbent dosage, pH, temperature and shaking speed applied were 4 mg/L, 0.1 (g/L), 7, 25°C and 150 rpm, respectively. All samples were separated from magnetite nanoparticles using magnet and 0.25 µm syringe filters.

3.5.6. Adsorption Kinetics

To examine the kinetics of levofloxacin removal the adsorbent mass was calculated according to levofloxacin solution and obtained optimum dose. The adsorbent mass calculated was used as dosage in this experiment. The 500 mL antibiotic (levofloxacin) solution was prepared of 4 mg/ L concentration. 500 mL levofloxacin solution was particularly prepared to lessen the effect of sampling volume. Other experimental conditions remained the same as pH7, shaking speed, temperature was adjusted at, 150 rpm, 25 °C and experiment was conducted for 24 hours. Samples were collected at various time intervals (5, 10, 20, 40, 60, 120, 240 and 1440 mins). Samples were collected, separated, and analyzed by HPLC.

3.5.7. Adsorption isotherm

Adsorption isotherm of levofloxacin removal was determined by conducting experiments using six different concentrations of levofloxacin in line segment of 4 to 24 (4, 8, 12, 16, 20 and 24 mg/L). Other parameters such as dose, pH, and temperature applied were optimal ones. The pH was maintained with 0.1 M HCl and 0.1 NaOH. The experiment was conducted for 24 hrs at 150 rpm and sample was collected after 24

hrs. Before analyzing on HPLC, sample was separated from nanoparticles using magnet and 0.25 µm syringe filters.

3.6. Statistical Analysis

For data analysis, removal efficiency and adsorption capacity were analyzed by the following equations (2) (Aydin et al., 2019) and (3) (Zhang et al., 2016), respectively.

$$\textbf{\textit{Removal efficiency}}\ (\%) = \frac{C_0 - C_e}{C_0} \times 100 \qquad \textbf{Equation (2)}$$

$$Q_e = (C_0 - C_e) \times \frac{\textit{volume of solution}}{\textit{mass of adsorbent}} \qquad \textbf{Equation (3)}$$

Where:

C_0 = Initial concentration of antibiotic (mg/L)

C_e = Equilibrium concentration of antibiotic (mg/L)

Q_e = Adsorption capacity (mg/g)

Adsorption capacity is the antibiotic amount adsorbed on the magnetite.

In the kinetic study, antibiotic adsorbed amount was calculated by using equation (4) (Altaf et al., 2021).

$$Q_t = \frac{(C_0 - C_t) \times V}{M} \qquad \textbf{Equation (4)}$$

Where:

Q_t = Adsorbed amount of antibiotic (mg/g)

C_0 = initial concentration of antibiotic (mg/L)

C_t = Concentration of antibiotic at time t (mg/L)

V = Volume of antibiotic solution (mL)

M = Adsorbent mass (g)

To investigate the kinetic mechanism behind the removal of antibiotics, results obtained from kinetic experiment were further analyzed via fitting of two models through equation (5) (Weber and Morris., 1963) and (6) (Ho and Mckay, 1999).

- Pseudo first-order model:

$$ln(Q_e - Q_t) = lnQ_e - K_1 t \qquad \textbf{Equation (5)}$$

1. Pseudo second-order model:

$$\frac{t}{Q_t} = \frac{1}{K_2 Q_e^2} + \frac{t}{Q_e} \qquad \textbf{Equation (6)}$$

Where:

K_1 = pseudo first order rate constant (mg/L. min)

K_2 = pseudo second order rate constant (mg/L. min)

The value of Q_e and K were calculated from the slope and intercept of the plotted straight line of both models, respectively (Yoon et al., 2014).

To determine mechanism of adsorption isotherm, the isotherm experiment data was analyzed by fitting of two isotherm models namely, Langmuir and Freundlich model using equation (7) (Langmuir., 1916; Hatt et al., 2013) and (9) (Gupta et al., 2010). Langmuir constant for separation factor was calculated by equation (Stan et al., 2017).

2. Langmuir model:

$$\frac{C_e}{Q_e} = \frac{1}{(Q_{max} \times K_L)} + \frac{C_e}{Q_{max}} \qquad \textbf{Equation (7)}$$

Where:

Q_{max} = Maximum adsorption capacity (mg/g)

K_L = Langmuir constant for adsorption energy and adsorption capacity.

$$R_L = \frac{1}{1+K_L C_0} \qquad \textbf{Equation (8)}$$

R_L = Langmuir constant for separation factor

3. Freundlich model

$$\log Q_e = \log K_f + \left(\frac{1}{n}\right) \log C_e \qquad \textbf{Equation (9)}$$

K_f = Freundlich constant for adsorption capacity (mg/L)

n = Freundlich constant for intensity of adsorption

All statistical analysis was conducted using Microsoft Excel, Origin Lab 9.65, SPSS.

Chapter 4

Results and Discussion

4.1. Magnetite nanoparticles synthesis and characterization

Characterization comparison of both green and chemically synthesized iron oxide nanoparticles confirmed that there was no major difference between green and chemically synthesized magnetite. Nanoparticles' yield was higher by green synthesis as it was 4.5 g per batch as compared to coprecipitation method which yielded 0.8 g per batch. The characterization results in detail are given below.

4.1.1. Morphological structure

Morphological structure of prepared magnetite was determined using SEM as shown in Figure 4.1 and 4.2. Some irregular, spherical, and polyhedral particles can be observed in SEM images of both chemically and gINPs. In green synthesis, it is ascribed to the polyphenols' presence on nanoparticles surface and magnetism reduction degree on their surface (Babuponnusami and Muthukumar., 2012; Kuang et al., 2013).

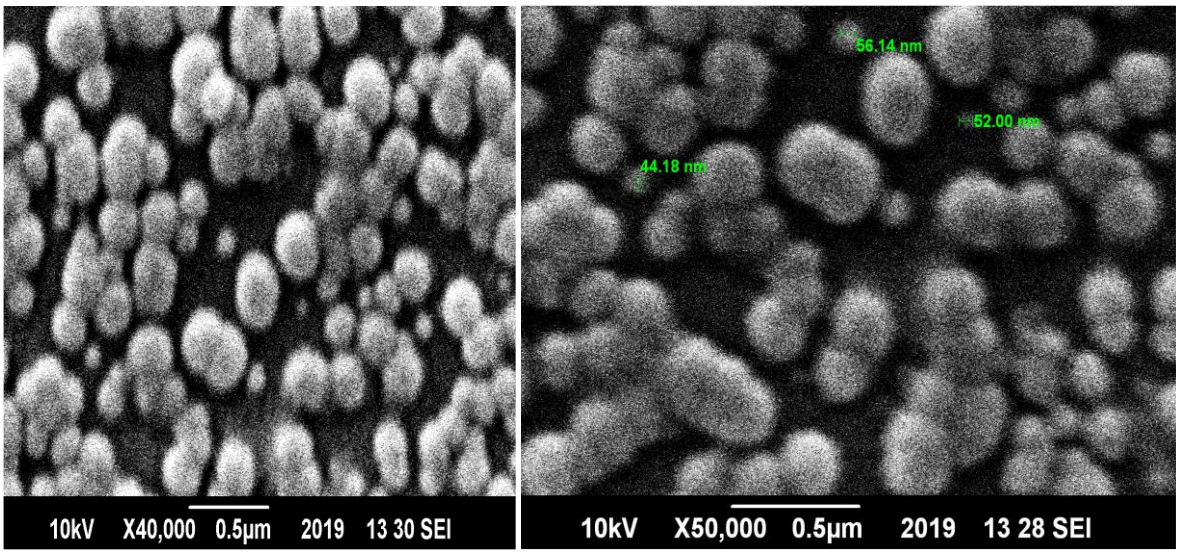

Figure 4.1. SEM images of green synthesized magnetite nanoparticles (gINPs)

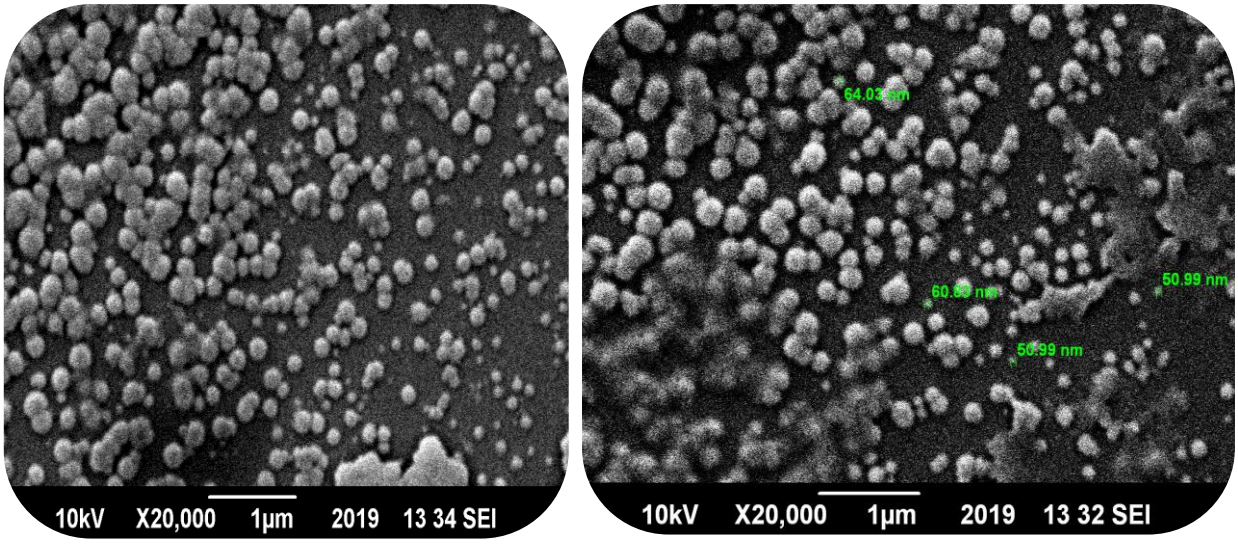

Figure 4.2. SEM images of chemically synthesized magnetite nanoparticles

4.1.2. XRD Analysis

In this study, purpose of XRD analysis was to scrutinize the crystallinity, phase purity and crystallite size. The crystalline structure of prepared magnetite is demonstrated in Figure 4.3. Characteristic peaks of green synthesized magnetite were described by 18.2°, 30.07°, 35.5°, 43.05°, 53.4°, 56.9° and 62.5° and these were same in chemically synthesized magnetite. Yazdani and Seddigh et al. (2016) reported the same characteristic peaks in magnetite synthesized by coprecipitation method. In the current study, the magnetite (Fe_3O_4) was existed as confirmed by the XRD spectrum and characteristics peaks. When XRD pattern was analyzed on Match (XRD analysis software), its spectrum matched with magnetite and its PDF number is given in Figure 4.3. Using the XRD spectrum crystallite size was calculated which shows that average crystallite size of gINPs was 14.34 nm and chemically synthesized was of 18.93 nm. Crystallite size conforms with particle size obtained using SEM. The data related to crystallite size calculations is given in Table 4.1 and 4.2.

Table 4.1. Crystallite size of gINPs

FWHM	Peak Positions	Crystallite Size (D)	Average Crystallite Size (D) (nm)
14.96	30.7	5.50	
6.96	35.3	11.97	14.34
9.91	42.9	8.60	

5.50	53.3	16.13
2.30	57.2	39.28
20.38	62.2	4.55

Table 4.2. Crystallite size of chemically synthesized nanoparticles (CINPs)

FWHM	Peak Position	Crystallite Size (D)	Average Crystallite Size (D) (nm)
6.95	30.4	11.82	18.93
2.71	35.6	30.71	
9.28	43.2	9.20	
6.36	53.3	13.97	
5.68	56.4	15.85	
2.90	62.7	32.04	

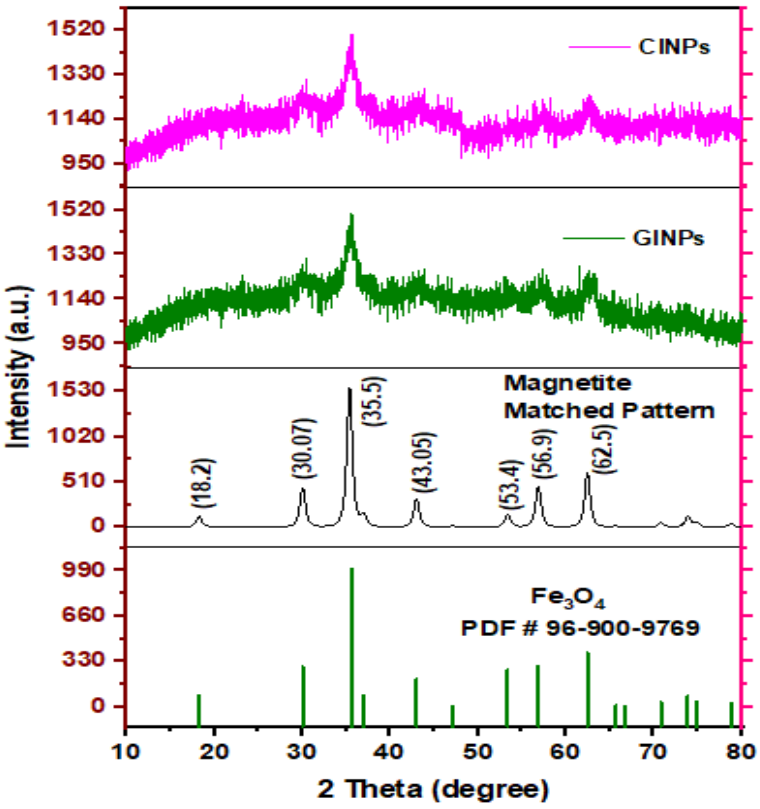

Figure 4.3. XRD pattern of magnetite nanoparticles

4.1.3. Fourier transform infrared (FTIR) spectra

FTIR spectra of prepared magnetite is illustrated in Figure 4.4. FTIR result showed similar spectra and functional groups in both green and chemically synthesized nanoparticles. The functional groups existed on particles surface are given with frequencies for green and chemically synthesized particles in Tables 4.3 and 4.4, respectively.

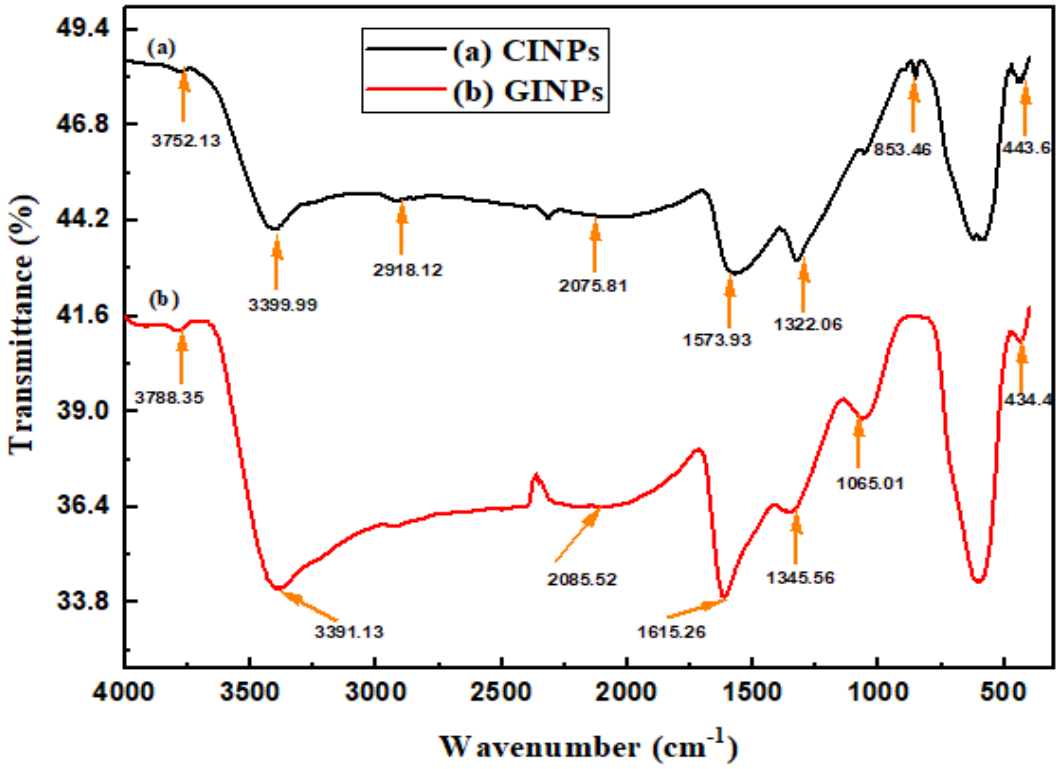

Figure 4.4. FTIR spectra of magnetite nanoparticles

The magnetite nanoparticles can be characterized by the bands; both 434.4 cm^{-1} and 443.6 cm^{-1} (magnetite) and 1345.5 cm^{-1} (maghemite) (Demirezen et al., 2019; Mazzetti and Thistlethwaite., 2002). Das et al. (2014) reported that the occurrence of magnetite can be recognized by the strong absorption band (434.4 cm^{-1}) and it correspond to the Fe-O stretching band of bulk magnetite (Fe_3O_4). Band 1615.2 cm^{-1} indicated the presence of flavonoids as Pompeu et al. (2018) reported that it is epicatechin which belong to flavonoid class. The band 3391.1 cm^{-1} also showed the O-H stretch which indicates the presence of polyphenols. These flavonoids and polyphenols must had contributed to the preparation of nanoparticles as may be these were found in *Moringa olifera* leaves.

Table 4.3. FTIR spectral bands of gINPs

Frequency (cm^{-1})	Bond	Functional Group
3391.1	O-H	Alcohols, Phenols
2085.5	C≡C	Alkynes
1615.2	O-H	Flavonoid
1345.5	Fe-O	Maghemite
434.4	Fe-O	Magnetite

Table 4.4. FTIR spectral bands of CINPs

Frequency (cm^{-1})	Bond	Functional Group
3399.1	O-H	Alcohol
2075.8	C=C	Aromatic Comp.
1573.9	O-H	water
1322.0	O-H	Water
443.6	Fe-O	Magnetite

4.2. Development of calibration curve

Different solutions of levofloxacin 10, 20, 30 and 40 mg/L were analyzed on HPLC at 280 nm, which gave the peak area of 465.51, 1190.43, 1763.59 and 2001.88, respectively. The standard curve was obtained with the R^2 of 0.9783. The sharp peaks of levofloxacin in chromatogram indicate its purity and retention time was 7.22 at 280 nm. The standard curve of levofloxacin with trendline equation is given in Figure 4.5. This trendline equation was used to determine experimental samples' concentration.

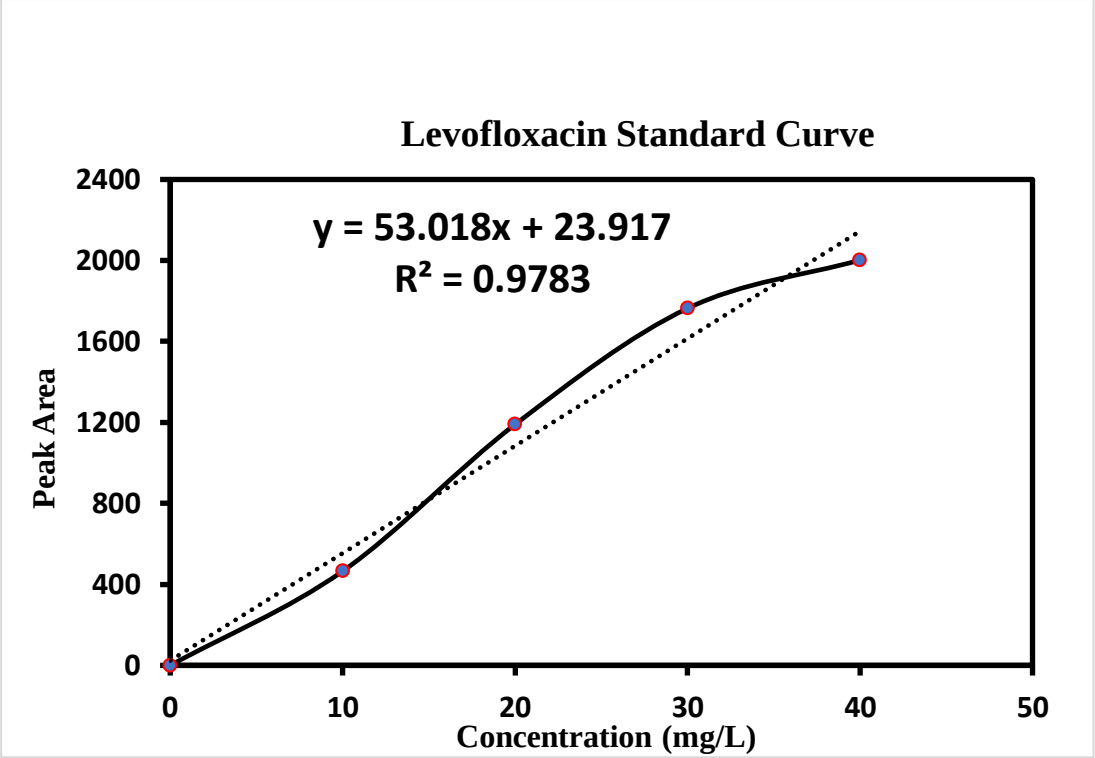

Figure 4.5. Levofloxacin calibration curve

4.3. Adsorption Experiments

Removal of levofloxacin was conducted in batch experiments at different conditions. Removal efficiency and adsorption capacity were calculated for levofloxacin removal under different conditions by gINPs using equation (2) and (3), respectively.

4.3.1. Effect of Magnetite Dosage

Adsorbent dosage effect on levofloxacin removal efficiency and adsorption capacity was observed as shown in Figure 4.6. The removal efficiencies of levofloxacin attained were 9.15, 10.95, 18.65, 22.56 and 81.07% at magnetite dosage of 0.005, 0.025, 0.050, 0.075, and 0.10 g L^{-1}, respectively. With increase of adsorbent dosage, there was increase of number of active sites and surface area which enhanced the removal efficiency. Mezenner and Bensmaili (2009) described that high dose of nanoparticles leads to aggregation of nanoparticles and significant number of adsorption binding sites which may result in high removal efficiency. Results of current study also confirmed that gINPs has more binding sites for antibiotic removal. Adsorption capacity also increased with the adsorbent dosage and increase of removal efficiency from 0.64 to 8.9 mg/g. It is higher at maximum dosage, because maximum number of binding sites

are filled, and it conforms with higher removal efficiency. Shukla et al. (2002) and Zhou et al. (2018) suggested that high adsorption capacity attributed to the fulfilling of most of the binding sites and increase in total surface area.

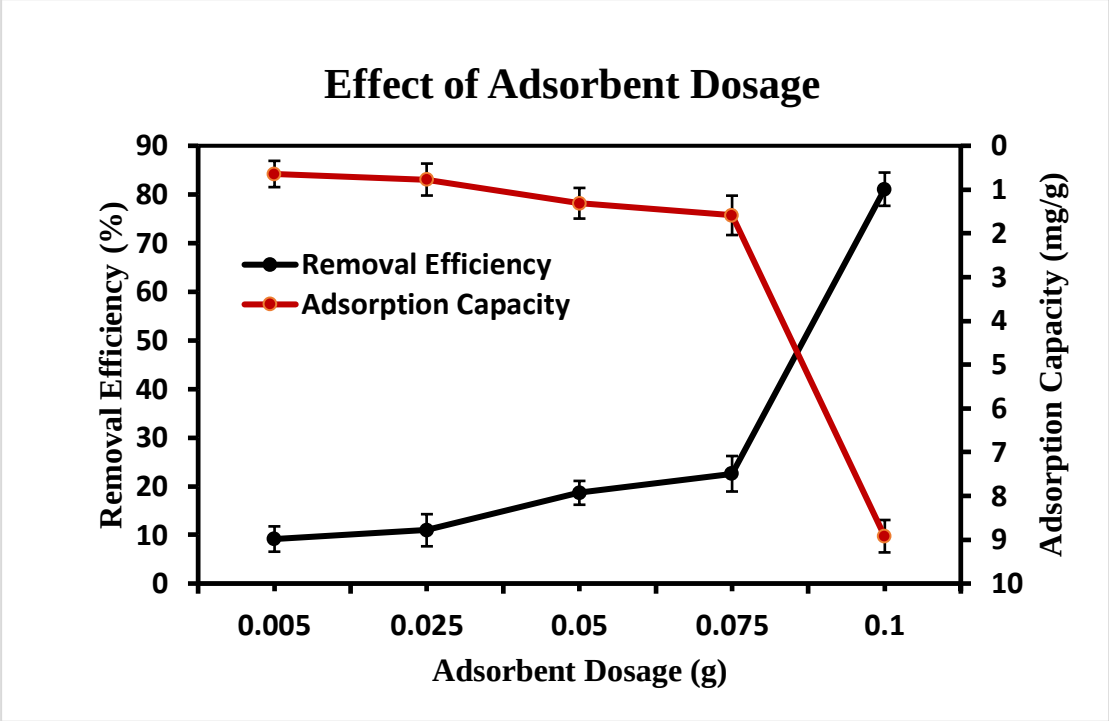

Figure 4.6. Effect of magnetite dosage (gINPs) on removal efficiency and adsorption capacity. Error bars show ± standard deviation values. Conditions: Levofloxacin initial concentration 4 mg/L, temp 25 °C, pH 6.45, time 24 h and shaking speed 150 rpm

4.3.2. Effect of adsorbate initial concentration

Levofloxacin concentration effect on adsorption capacity and removal efficiency is illustrated in Figure 4.7. The removal efficiencies attained were 82.36, 59.10, 43.29, 34.34 and 29.37% at levofloxacin initial concentration of 4, 8, 12, 16, 20 and 24 mg/L, respectively. Removal efficiency of gINPs was decreased along with increase of adsorbate initial concentration. It can be attributed to the fixed amount of adsorbent dosage in this experiment. Every adsorbent has restricted number of binding sites which may lead to saturation of them after certain amount of adsorbate (Weng et al., 2013; Pouretedal and Sadegh., 2014). Adsorption capacity decreased with decreasing removal efficiency and increasing adsorbate initial concentration from 9.7 to 2.1. Levofloxacin initial concentration overwhelmed the resistance to bulk transfer between the liquid phase of adsorbate and adsorbent solid phase by vital driving force. The increase in

initial concentration of levofloxacin enhanced the interaction between adsorbate and adsorbent. This is because of higher driving force of concentration gradient with high adsorbate concentration (Shirzad Siboni et al., 2011; Kumar et al., 2010).

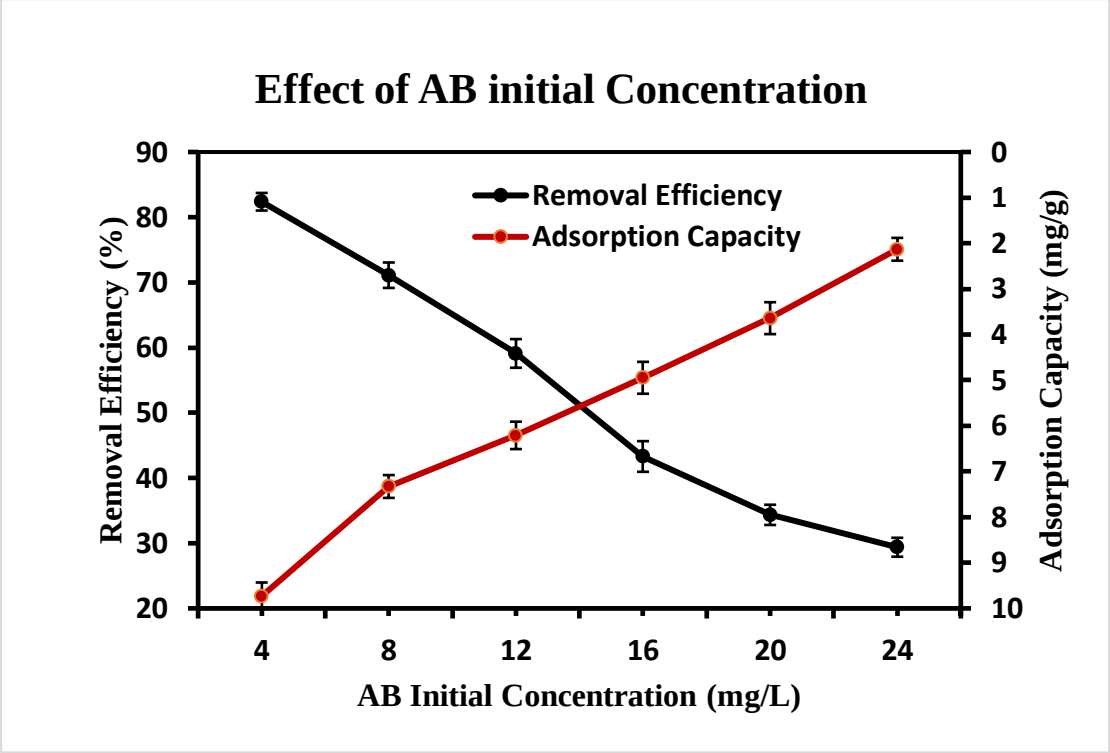

Figure 4.7. Effect of adsorbate (levofloxacin) initial concentration on removal efficiency and adsorption capacity. Error bars show ± standard deviation values. Conditions: gINPs 0.10 g/L, time 24 h, temp 25 °C, pH 6.55 and shaking speed 150 rpm

4.3.3. Effect of solution initial pH

The effect of pH of antibiotic solution is essential in adsorption study for determination of optimal pH on which maximum adsorption occurs. The removal of levofloxacin by green synthesized magnetite at different pH values of 4 to 10 is shown in Figure 4.8. The removal efficiency calculated were 66.28, 70.28, 73.70, 81.44, 77.57, 66.96 and 64.39% at pH of 4, 5, 6, 7, 8, 9 and 10, respectively. The results indicated that at pH 7, gINPs uptake of levofloxacin was higher than that at acidic and alkaline pH. Adsorption capacity showed the direct relation with the removal efficiency at pH 7, that was maximum. The pKa1 and pKa2 values of Levo are 6.02 and 8.74, respectively (Swan et al., 1983; Torniainen et al., 1996). So, at pH 7, levofloxacin existed as zwitterion/neutral form which makes its dissociation and interaction with adsorbent (gINPs) easier. The removal efficiency and adsorption capacity decreased as pH

decreased (become acidic) or increased (alkaline) because of electrostatic repulsion among similar charges (Wallaice et al., 1996; Wu et al., 2010). The pH dependent structure of levo is shown in Figure 4.9 (A-Jabri et al., 2019). The affinity of metal ions adsorbent with some fluoroquinolone cationic and anionic adsorbate is weaker than their zwitterionic/neutral counterpart and it may be attributed to the results of pH other than neutral (Li et al., 2017). Iron oxide nanoparticles make passive oxide layer by precipitating on surface at alkaline pH which may slower the uptake of levofloxacin by metallic core (Rezaei and Vione, 2018).

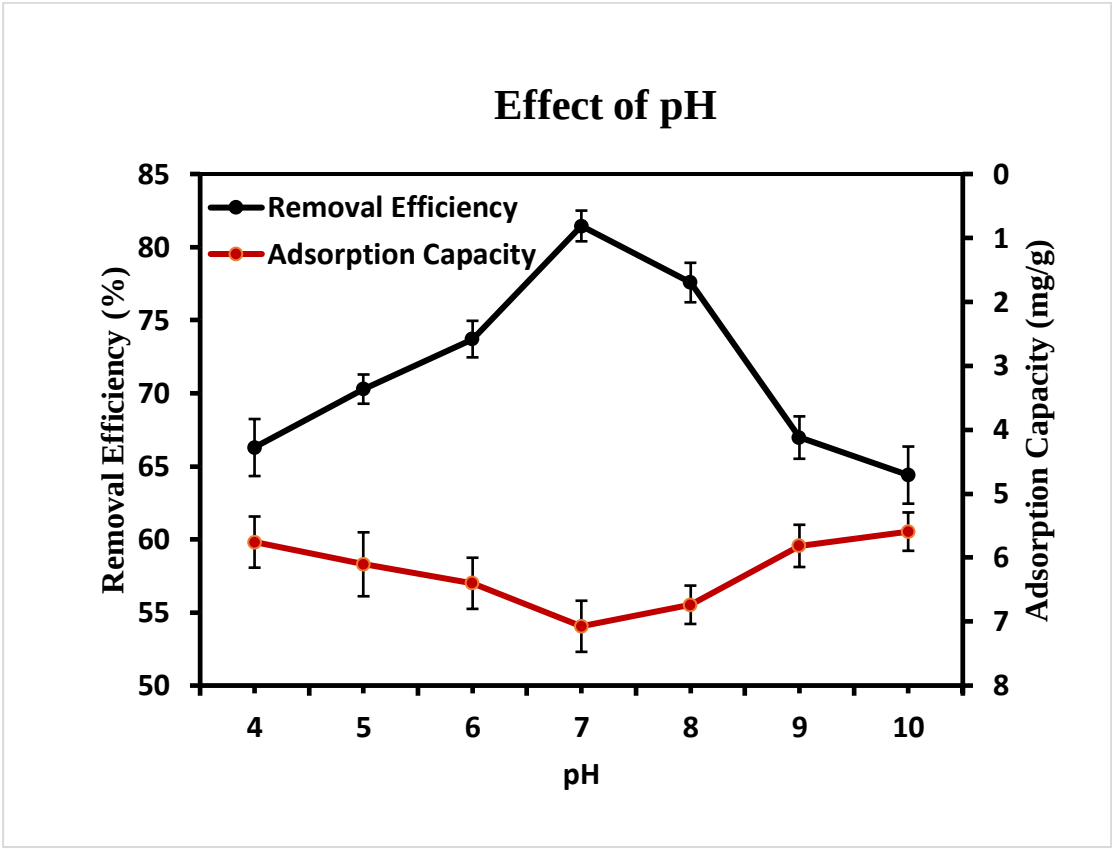

Figure 4.8. Effect of solution initial pH on removal efficiency and adsorption capacity. Error bars show ± standard deviation values. Conditions: gINPs 0.10 g/L, levofloxacin 4 mg/L, temp 25 °C, time 24 hand shaking speed 150 rpm

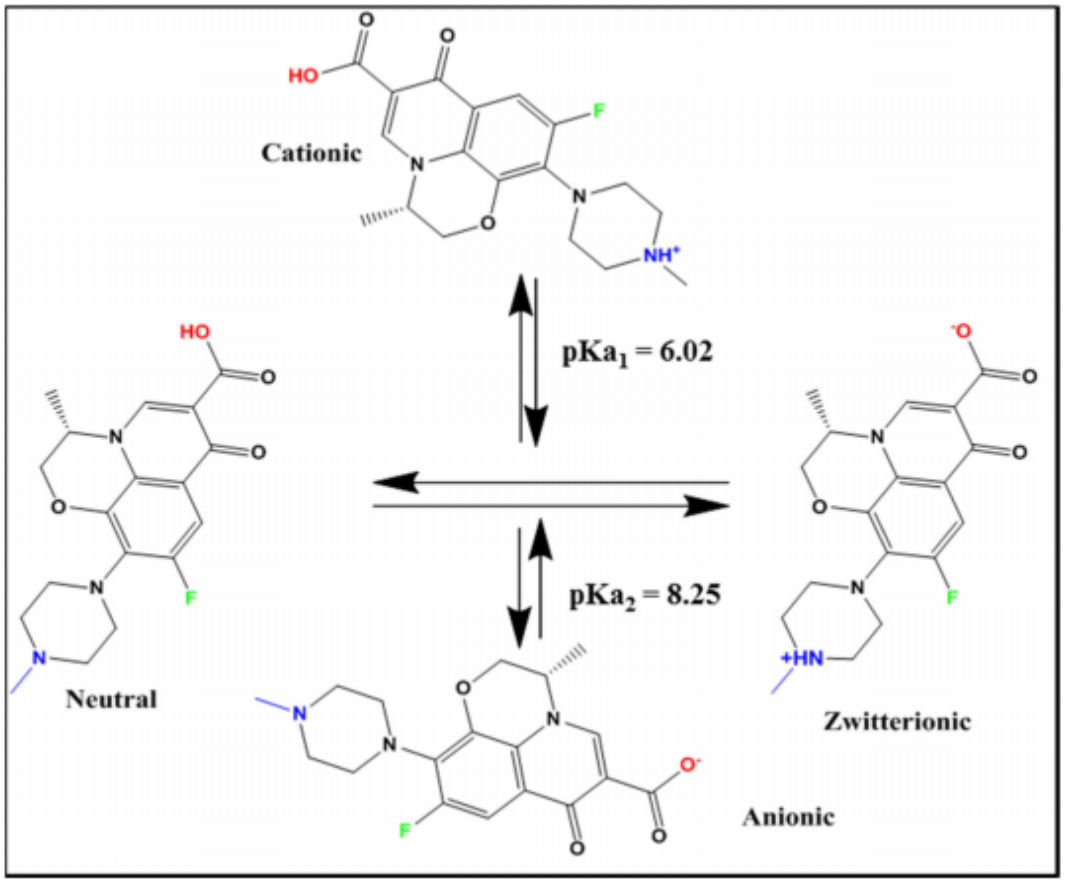

Figure 4.9. pH dependent structure of Levo (Al-Jabri et al., 2019)

4.3.4. Effect of temperature

The removal efficiency and adsorption capacity of levofloxacin by gINPs at various temperatures are exhibited by Figure 4.10 (a) and (b), respectively. Results showed that maximum removal efficiency and adsorption capacity were achieved by optimal adsorbate concentration and at 25 °C. There was no major difference between the removal efficiency calculated at four different temperatures between 20 to 35 °C. But all adsorbate concentrations showed the same order of removal efficiency and adsorption capacity. The maximum removal efficiency calculated for 4 mg/L concentration was 76.84, 84.19, 79.9 and 75.99% at temperature of 20, 25, 30 and 35 °C, respectively. At lower temperature, both removal efficiency and adsorption capacity increased because of active sites expansion which increased interaction between them and levofloxacin. The higher removal efficiency is also due to easy C-N bond break down at given temperature. But at higher temperature, adsorbate uptake

decreased because of higher updraft movement of molecules of adsorbate, it reduced the attraction between active sites and antibiotics (Turku et al., 2007; Chen et al., 2011)

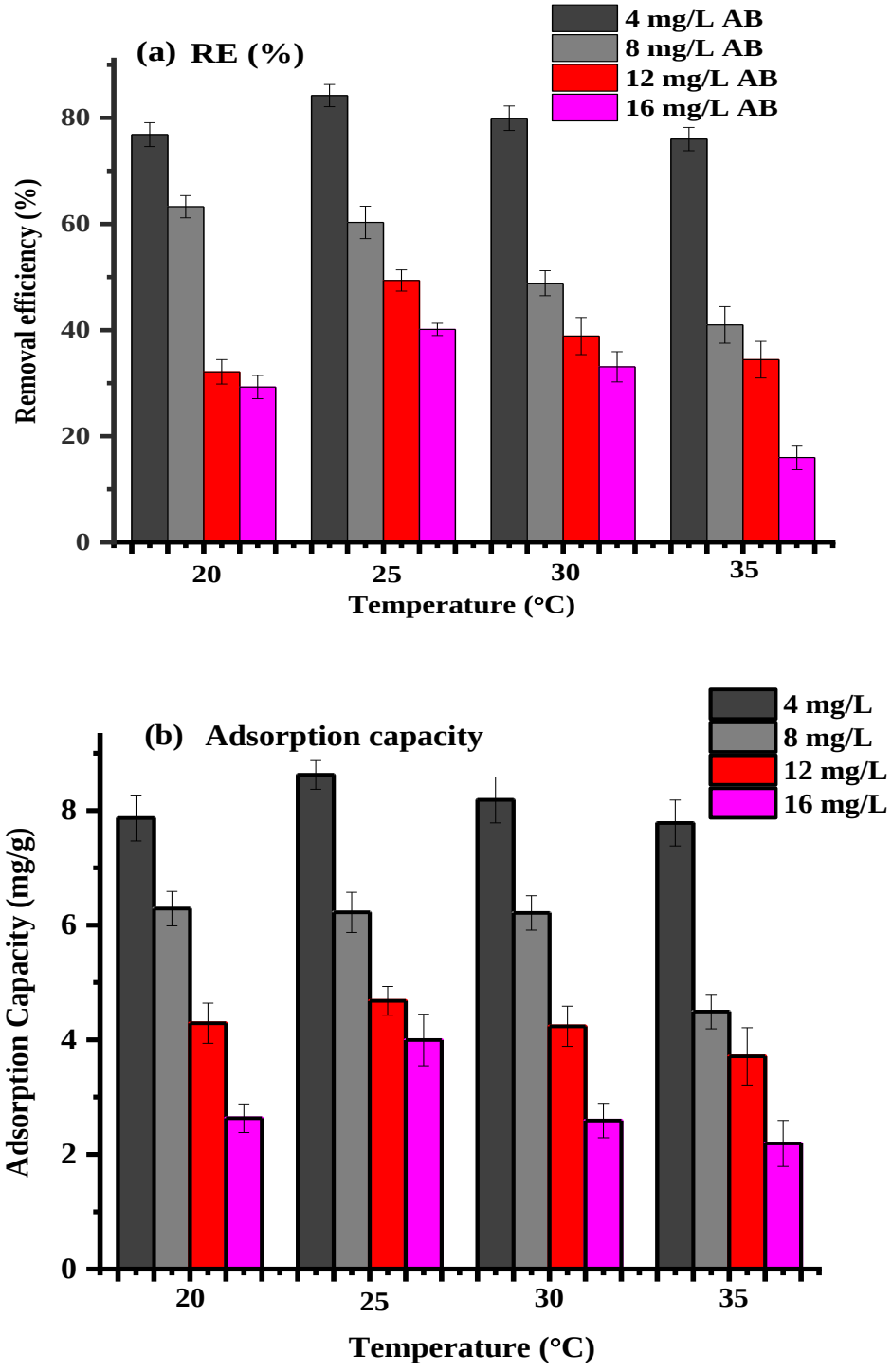

Figure 4.10. Effect of temperature on removal efficiency (a) and adsorption capacity (b). Error bars show ± standard deviation values. Conditions: time 24 h, gINPs 0.10 g/L, pH 7, and shaking speed 150 rpm

4.3.5. Effect of contact time

Removal of levofloxacin by green synthesized magnetite at different time intervals is shown in Figure 4.11.

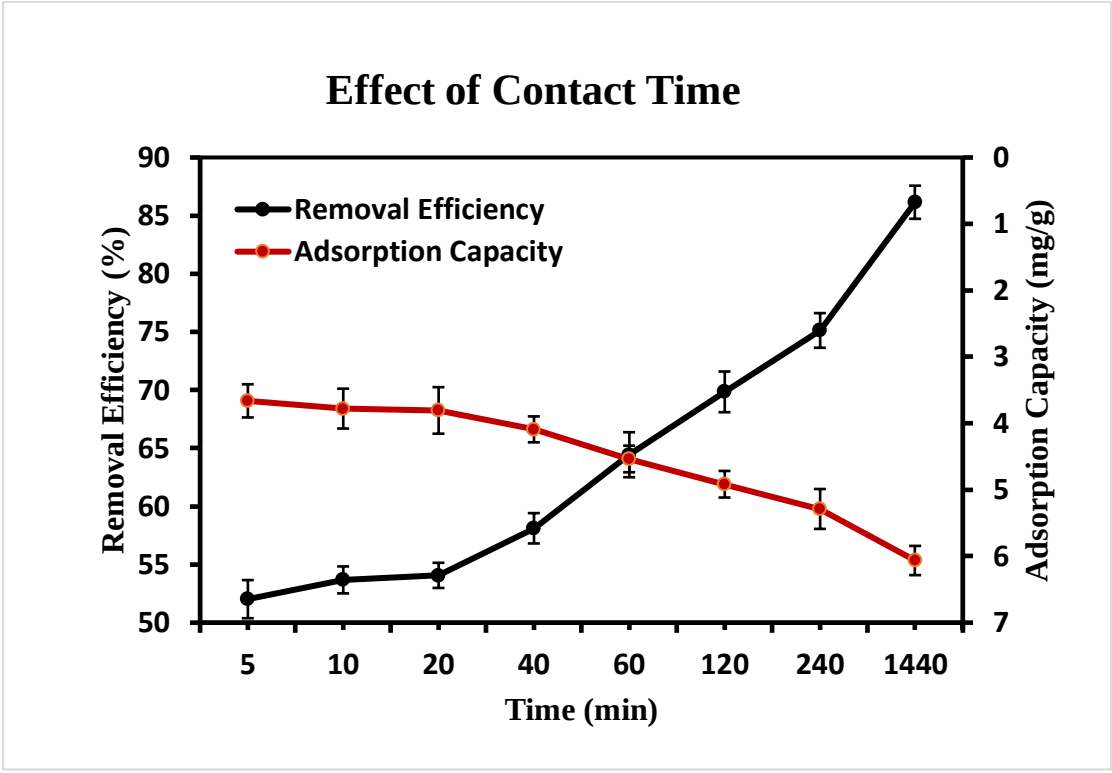

Figure 4.11. Effect of contact time on removal efficiency and adsorption capacity. Error bars show ± standard deviation values. Conditions: gINPs 0.10 g/L, levofloxacin 4 mg/L, temp 25 °C, pH 7, time 24 h, and shaking speed 150 rpm

Levofloxacin uptake by gINPs was significantly high in the beginning of experiment but after 40 min, it was slowed and achieved equilibrium in 24 hrs. The fast uptake was due to availability of a larger number of binding sites and concentration gradient. Maximum removal efficiency and adsorption capacity achieved after 24 hrs was 86.15% and 9.09 mg/g, respectively. The gradual increase of antibiotic uptake (adsorption), and subsequently, the achievement of equilibrium point may be attributed to molecules' limited mass transfer from the immense solution of adsorbate to gINPs exterior initially, but internal mass transfer became slower into core of nanoparticles (Kumar et al., 2010). Chang et al. (2009) suggested that after a time interval, the repulsive force generated between adsorbent and liquid bulk of adsorbate because of unavailability of binding sites for adsorption. But it might have occurred because of

controlled attachment process. When external sites were exhausted, uptake rate of adsorbate was determined by the rate of transfer of bulk liquid into core.

4.4. Adsorption kinetics and mechanism

Dynamics of reaction were identified with the help of kinetic study. The results of fitting of kinetic data constructed by equation 5 and 6 are illustrated by Figure 4.12 and Table 4.5. The levofloxacin adsorbed amount (Q_t) was increased with increasing contact time beginning from 5 min to 1440 min. Figure 4.12 (a) pseudo first order and (b) pseudo second order indicate that at the beginning, the uptake of levofloxacin by gINPs was rapid and then reached at equilibrium in 1440 min. The increase of antibiotic adsorption efficiency was due to availability of binding sites. Table 4.5 shows that pseudo second-order model with high correlation coefficient (R^2 = 0.965) was better fitted as comparison to pseudo first-order model (R^2 = 0.964). The applicability of pseudo second order means the process involved in kinetic adsorption was chemisorption, but the R^2 value of pseudo first order is also near R^2 of pseudo second order which described that with chemisorption, diffusion process was also involved (Huang et al., 2020). In chemisorption, the chemical bonds were formed between adsorbate and adsorbent, and adsorbate tended to get sites that maximized their coordination number with surface (Atkins., 1995). If chemisorption was involved, it means gINPs had a lot of active sites for chemisorption and it was promoted by electrical charges by shifting ionization energy and electron affinities (Schmidt et al., 2015). The lower value of adsorption constants is indicating that process was exothermic and had higher adsorption capacity (Da'na et al., 2018). Hence, the above data suggested that the process involved was chemisorption and exothermic.

Table 4.5. Kinetic models parameter for adsorption of Levo by gINPs

(a)

Pseudo first order		
K_1 (L/(mg.min))	**Q_e (mg/g)**	**R^2**
0.348	**4.429**	**0.964**

(b)

Pseudo second order		
K_2 (L/(mg.min))	**Q_e (mg/g)**	**R^2**
0.100	**8.831**	**0.965**

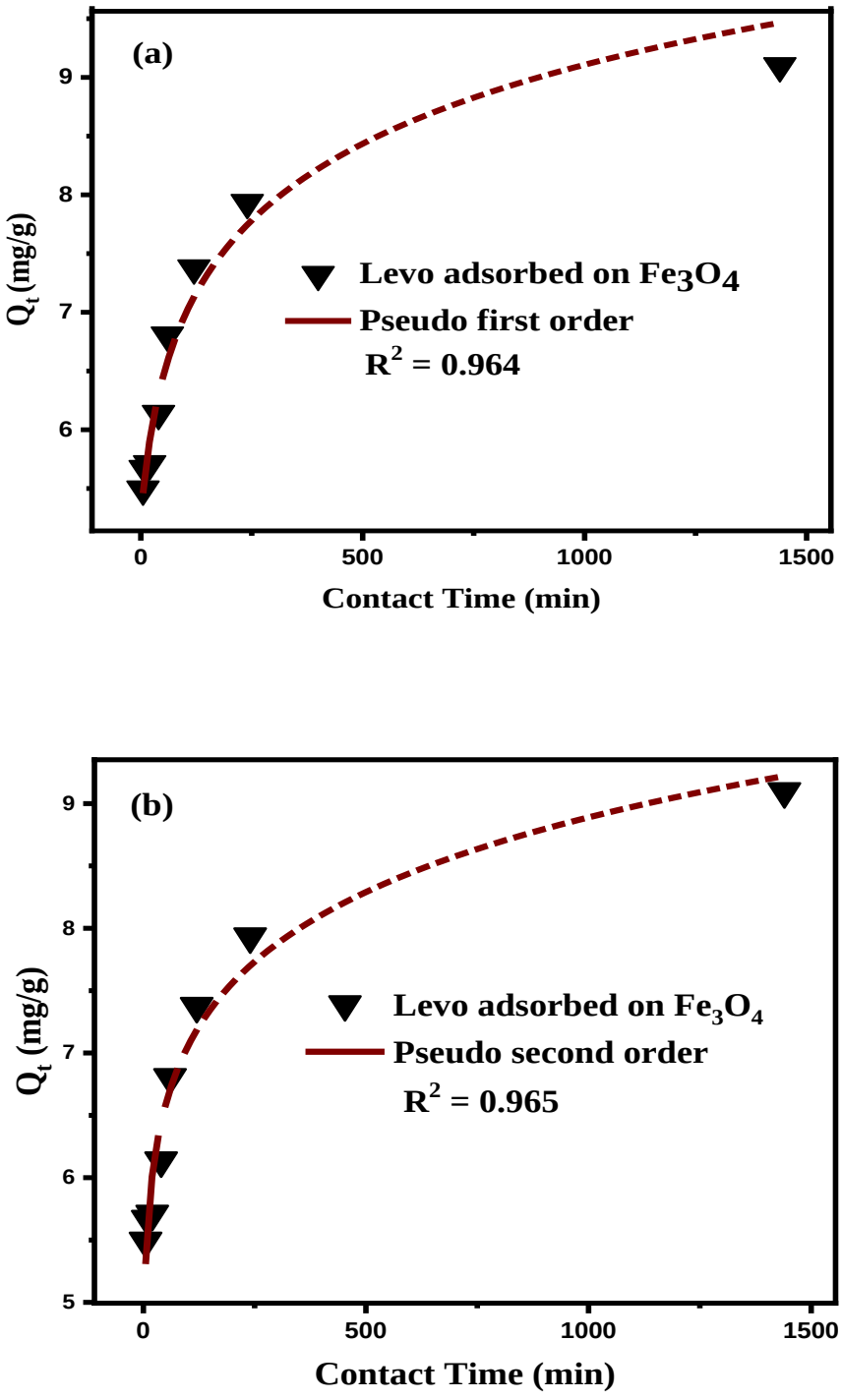

Figure 4.12. Fitted plots of kinetic models (a)pseudo first- order, and (b) pseudo second- order for levofloxacin adsorption by gINPs . Conditions: time 24 h, pH 7, temp 25 °C, sand shaking speed 150 rpm.

4.5. Adsorption equilibrium Isotherm

To determine the interaction between gINPs surface and antibiotic molecules, equilibrium isotherm models were applied. Figure 4.13 (a) Langmuir model and (b) Freundlich model showed that experimental data was well fitted by both models, respectively. For simulating levofloxacin adsorption capacity, both Langmuir and Freundlich seemed to be suitable rendering to good correlation coefficient R^2 = 0.993 and 0.994, respectively. But it was better explained by Freundlich isotherm which showed that adsorption was heterogenous, monolayer and, multilayer and non-uniform surface of the adsorbent (Al-Jabri et al., 2019). Kumar et al. (2010) reported the well-fitting of both models for Pb^{+2} adsorption by Nano silver-sol coated activated carbon with correlation coefficient of 0.997 and 0.998, respectively. Maximum adsorption capacity (Q_{max}) of gINPs obtained from Langmuir model was 22.47 mg/L. The value of Langmuir separation factor (R_L) is slightly higher than 1 which shows that antibiotic may easily be separated from wastewater and Langmuir model may be applicable (Stan et al., 2017). But the 1/n is the adsorption intensity which explains heterogeneity of adsorbent and relative energy distribution. The 1/n value is less than one in this study which shows that adsorption was favorable chemical process. So, from the evidence, best fitted model for equilibrium isotherm was Freundlich isotherm. Results of isotherm model fitting of experimental data are provided in Table 4.6.

Table 4.6. The Langmuir and Freundlich isotherm model parameters for adsorption of Levo using gINPs

(a)

Langmuir Model			
Q_{max} (mg/g)	**K_L (mg/L)**	**R_L**	**R^2**
22.47	**0.01**	**1.04**	**0.993**

(b)

Freundlich Model		
K_f (mg/L)	**1/n**	**R^2**
26.63	**0.831**	**0.994**

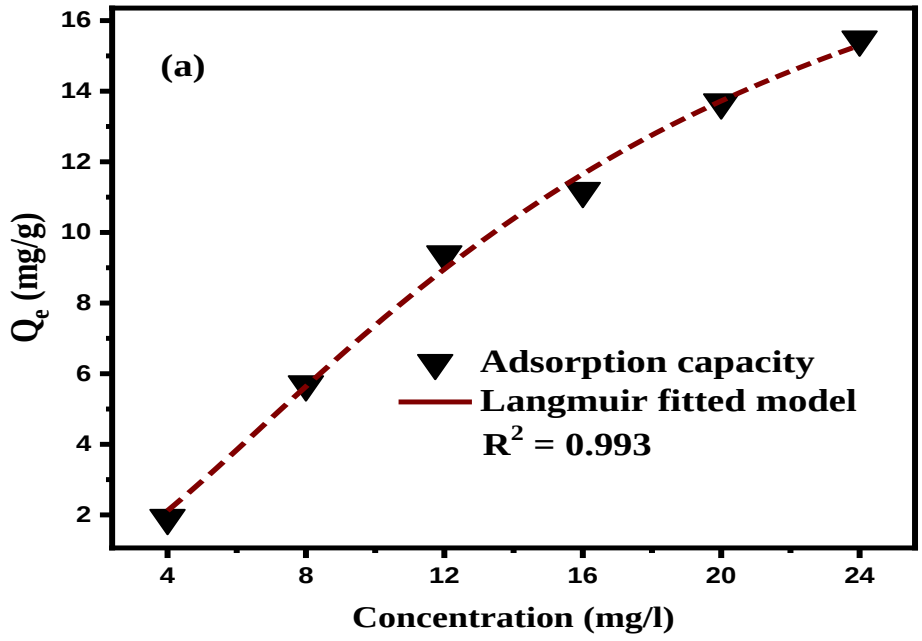

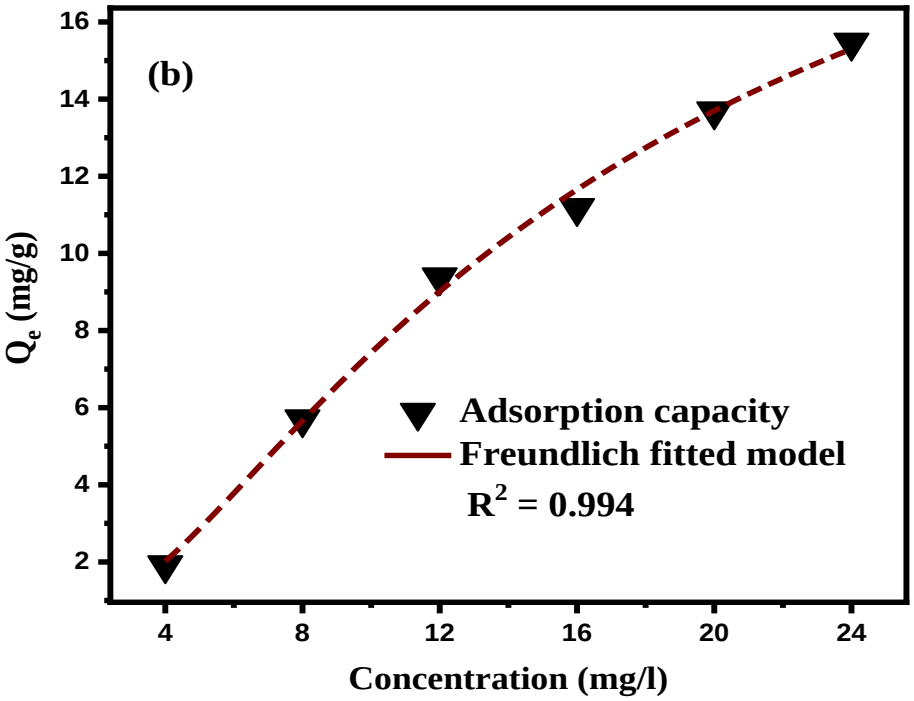

Figure 4.12. Fitted plots of Langmuir model (a), and Freundlich model (b) for levofloxacin adsorption by gINPs . Conditions: time 24 h, pH 7, temp 25 °C, and shaking speed 150 rpm.

Chapter 5

Conclusions and Recommendations

5.1. Conclusions

Current study investigated the green synthesis of magnetite (Fe_3O_4) using *Moringa olifera* leaves and using it for antibiotics (levofloxacin) removal. The synthesis of gINPs was confirmed by comparison with characterization of magnetite prepared by coprecipitation method and compound existed in XRD of gINPs was magnetite (Fe_3O_4). Nanoparticles' yield using green method was higher than coprecipitation method. The results showed that gINPs were effective for levofloxacin removal from wastewater. The respective maximum adsorption capacity for levofloxacin calculated by Freundlich model was 26.63 mg/g, attained at equilibrium stage. Chemisorption mechanism and exothermic process was suggested by pseudo second order ($R^2 = 0.965$) while the chemical, monolayer and heterogenous adsorption mechanism was recommended by Langmuir and Freundlich models with R^2 0.993 and 0.994, respectively. The maximum removal efficiency achieved was 86.15% during 24 h at optimal conditions. The removal efficiency and adsorption capacity increased with adsorbent dosage. The presented results reveal that gINPs can successfully be used for antibiotics removal. The synthesis of magnetite using *Moringa olifera* or other plant extracts is advantageous as it is fast, cost-effective, energy efficient, environment-friendly, economical, and easy to operate.

5.2. Recommendations

With increasing trend of antibiotics production, consumption and release into environment, antibiotic removal techniques would get more attention in coming years. Based on results of current study, some recommendations for future research are as under:

1. More studies should be conducted on the presence of antibiotics in different environmental compartments as there is lack of data in this direction.
2. More research is needed in the field of antibiotics removal from wastewater to have an effective strategy.
3. Different chemicals can be obtained other than iron oxide using plant extract and their efficiency for antibiotics removal can be examined.

4. Behavior of other antibiotics in wastewater and their removal kinetics can also be studied.
5. Adsorption technology alone is not sufficient for antibiotics removal, so it must be combined with any other technology to completely remove antibiotics.
6. Policy makers could be acquainted with the methods of antibiotic removal while emphasizing research in the said domain.
7. There is need for making environmental laws, standards for antibiotics and their implementation.

References

Ali, I., Afshinb, S., Poureshgh, Y., Azari, A., Rashtbari, Y., Feizizadeh, A., & Fazlzadeh, M. **(2020)**. Green preparation of activated carbon from pomegranate peel coated with zero-valent iron nanoparticles (nZVI) and isotherm and kinetic studies of amoxicillin removal in water. *Environmental Science and Pollution Research*, *27*(29), 36732-36743.

Al-Jabari, M. H., Sulaiman, S., Ali, S., Barakat, R., Mubarak, A., & Khan, S. A. **(2019).** Adsorption study of levofloxacin on reusable magnetic nanoparticles: Kinetics and antibacterial activity. *Journal of Molecular Liquids*, *291*, 111249.

Altaf, R., Lin, X., Tadda, M. A., Zhu, S., & Liu, D. **(2021).** Modified magnetite adsorbent (Zr–La@ Fe_3O_4) for nitrilo-tris-methylene-phosphonate (NTMP) removal and recovery from wastewater. *Journal of Cleaner Production*, *278*, 123960.

Arias, A., Alvarino, T., Allegue, T., Suárez, S., Garrido, J. M., & Omil, F. **(2018)**. An innovative wastewater treatment technology based on UASB and IFAS for cost-efficient macro and micropollutant removal. *Journal of Hazardous Materials*, *359*, 113-120.

Arshad, M., & Zafar, R. **(2020)**. Antibiotics, AMRs, and ARGs: fate in the environment. In *Antibiotics and Antimicrobial Resistance Genes in the Environment* (pp. 138-154). Elsevier.

Atkins, P. W., Physical Chemistry. 5th Edition, Oxford. Oxford University Press **(1995)**.

Aydin, S., Aydin, M. E., Ulvi, A., & Kiliç, H. **(2019)**. Antibiotics in hospital effluents: occurrence, contribution to urban wastewater, removal in a wastewater treatment plant, and environmental risk assessment. *Environmental Science and Pollution Research, 26*(1), 544–558.

Babuponnusami, A., & Muthukumar, K. **(2012)**. Removal of phenol by heterogenous photo electro Fenton-like process using nano-zero valent iron. *Separation and Purification Technolology*, 98, 130–135.

Batt, A. L., Kim, S. & Aga, D. S. **(2007)**. Comparison of the occurrence of antibiotics in four full-scale wastewater treatment plants with varying designs and operations. *Chemosphere* 68(3): 428-435.

Bielen, A., Šimatović, A., Kosić-Vukšić, J., Senta, I., Ahel, M., Babić, S., & Udiković-Kolić, N. **(2017)**. Negative environmental impacts of antibiotic-contaminated effluents from pharmaceutical industries. *Water Research*, *126*, 79-87.

Bolan, N. S., Szogi, A. A., Chuasavathi, T., Seshadri, B., Rothrock Jr, M. J., & Panneerselvam, P. **(2010)**. Uses and management of poultry litter. *World's Poultry Science Journal*, *66*(4), 673-698.

Brenner, C. G. B., Mallmann, C. A., Arsand, D. R., Mayer, F. M., & Martins, A. F. **(2010)**. Determination of sulfamethoxazole and trimethoprim and their metabolites in hospital effluent. *Clean-Soil, Air, Water, 39*(1), 28–34.

Brown, K. D., Kulis, J., Thomson, B., Chapman, T. H., & Mawhinney, D. B. **(2006)**. Occurrence of antibiotics in hospital, residential, and dairy effluent, municipal wastewater, and the Rio Grande in New Mexico. *Science of the Total Environment*, *366*(2-3), 772-783.

Chang, P. H., Li, Z., Yu, T. L., Munkhbayer, S., Kuo, T. H., Hung, Y. C., & Lin, K. H. **(2009).** Sorptive removal of tetracycline from water by palygorskite. *Journal of Hazardous Materials*, *165*(1-3), 148-155.

Chen, Z. X., Jin, X. Y., Chen, Z., Megharaj, M., & Naidu, R. **(2011).** Removal of methyl orange from aqueous solution using bentonite-supported nanoscale zero-valent iron. *Journal of Colloid and Interface Science*, *363*(2), 601-607.

Cheng, N., Wang, B., Wu, P., Lee, X., Xing, Y., Chen, M., & Gao, B. **(2021)**. Adsorption of emerging contaminants from water and wastewater by modified biochar: A review. *Environmental Pollution*, 116448.

Da'na, E., Taha, A., & Afkar, E. **(2018)**. Green synthesis of iron nanoparticles by *Acacia nilotica* pods extract and its catalytic, adsorption, and antibacterial activities. *Applied Sciences*, *8*(10), 1922.

Das, A.K., Marwal, A., & Verma, R. **(2014)**. *Datura inoxia* leaf extract mediated one step green synthesis and characterization of magnetite (Fe_3O_4) nanoparticles. Res. Rev.: *Journal of Pharmaceutical and Technology*, 2, 21–24.

Deegan, A. M., Shaik, B., Nolan, K., Urell, K., Oelgemöller, M., Tobin, J., & Morrissey, A. **(2011)**. Treatment options for wastewater effluents from pharmaceutical companies. *International Journal of Environmental Science & Technology*, *8*(3), 649-666.

Demirezen, D. A., Yıldız, Y. Ş., & Yılmaz, D. D. **(2019)**. Amoxicillin degradation using green synthesized iron oxide nanoparticles: Kinetics and mechanism analysis. *Environmental Nanotechnology, Monitoring & Management*, *11*, 100219.

Dinh, Q. T., Moreau-Guigon, E., Labadie, P., Alliot, F., Teil, M.-J., & Blanchard, M. **(2017)**. Fate of antibiotics from hospital and domestic sources in a sewage network. *Science of the Total Environment, 575*, 758–766.

Do, D.D. **(1998)** Adsorption analysis: Equilibria and kinetics, Imperial College Press

Dorival-García, N., Zafra-Gómez, A., Cantarero, S., Navalón, A., & Vílchez, J. L. **(2013)**. Simultaneous determination of 13 quinolone antibiotic derivatives in wastewater samples using solid-phase extraction and ultraperformance liquid chromatography–tandem mass spectrometry. *Microchemical Journal*, *106*, 323-333.

El-Maraghy, C. M., El-Borady, O. M., & El-Naem, O. A. **(2020)**. Effective removal of levofloxacin from pharmaceutical wastewater using synthesized zinc oxide, graphene oxide nanoparticles compared with their combination. *Scientific Reports*, *10*(1), 1-13.

Fan, N. S., Bai, Y. H., Chen, Q. Q., Shen, Y. Y., Huang, B. C., & Jin, R. C. **(2020)**. Deciphering the toxic effects of antibiotics on denitrification: Process performance, microbial community and antibiotic resistance genes. *Journal of Environmental Management*, *262*, 110375.

Fernandez, I., Mosquera-Corral, A., Campos, J. L., & Mendez, R. **(2009)**. Operation of an Anammox SBR in the presence of two broad-spectrum antibiotics. *Process Biochemistry*, *44*(4), 494-498.

Fick, J., Soderstrom, H., Lindberg, R. H., Phan, C., Tysklind, M., & Larsson, J. D. G. **(2009)**. Contamination of surface, ground, and drinking water from pharmaceutical production. *Environmental Toxicology and Chemistry, 28*, 2522–2527.

Gao, L., Shi, Y., Li, W., Liu, J., & Cai, Y. **(2015)**. Occurrence and distribution of antibiotics in urban soil in Beijing and Shanghai, China. *Environmental Science and Pollution Research*, *22*(15), 11360-11371.

Gardea-Torresdey, J. L., Gomez, E., Peralta-Videa, J. R., Parsons, J. G., Troiani, H., & Jose-Yacaman, M. **(2003)**. *Alfalfa sprouts*: a natural source for the synthesis of silver nanoparticles. *Langmuir*, *19*(4), 1357-1361.

Grandclément, C., Seyssiecq, I., Piram, A., Wong-Wah-Chung, P., Vanot, G., Tiliacos, N., & Doumenq, P. **(2017)**. From the conventional biological wastewater treatment to hybrid processes, the evaluation of organic micropollutant removal: a review. *Water Research*, 111, 297-317.

Granzoto, M. R., Seabra, I., Malvestiti, J. A., Cristale, J., & Dantas, R. F. **(2021)**. Integration of ozone, UV/H2O2 and GAC in a multi-barrier treatment for secondary effluent

polishing: reuse parameters and micropollutants removal. *Science of the Total Environment*, *759*, 143498.

Gulkowska, A., Leung, H. W., So, M. K., Taniyasu, S., Yamashita, N., Yeung, L. W., & Lam, P. K. **(2008)**. Removal of antibiotics from wastewater by sewage treatment facilities in Hong Kong and Shenzhen, China. *Water Research*, *42*(1-2), 395-403.

Guo, B., Gong, L., Duan, E., Liu, R., Ren, A., Han, J., & Zhao, W. **(2012)**. Characteristics of penicillin bacterial residue. *Journal of the Air & Waste Management Association*, *62*(4), 485-488.

Guo, X., Xiaojun, L., Zhang, A., Yan, Z., Chen, S., & Wang, N. **(2020)**. Antibiotic contamination in a typical water-rich city in southeast China: a concern for drinking water resource safety. *Journal of Environmental Science and Health, Part B*, *55*(3), 193-209.

Gupta, V. K., Rastogi, A., & Nayak, A. **(2010).** Biosorption of nickel onto treated alga (Oedogonium hatei): application of isotherm and kinetic models. *Journal of Colloid and Interface Science*, *342*(2), 533-539.

Hatt, J. W., Germain, E., & Judd, S. J. **(2013).** Granular activated carbon for removal of organic matter and turbidity from secondary wastewater. *Water Science and Technology*, *67*(4), 846-853.

Ho, Y.S., & McKay, G., **(1999).** Pseudo-second order model for sorption processes. *Process Biochemistry*. 34, 451e465. https://doi.org/10.1016/S0032-9592(98)00112-5.

http://www.pbs.gov.pk/.

Huang, Y., Lee, X., Grattieri, M., Yuan, M., Cai, R., Macazo, F.C., Minteer, S.D. **(2020).** Modified biochar for phosphate adsorption in environmentally relevant Conditions. *Chemical Engineering Journal*. 380, 122375.

Iakovides, I. C., Michael-Kordatou, I., Moreira, N. F., Ribeiro, A. R., Fernandes, T., Pereira, M. F. R., & Fatta-Kassinos, D. **(2019)**. Continuous ozonation of urban wastewater: Removal of antibiotics, antibiotic-resistant *Escherichia coli* and antibiotic resistance genes and phytotoxicity. *Water Research*, *159*, 333-347.

Ji, J. Y., Xing, Y. J., Ma, Z. T., Cai, J., Zheng, P., & Lu, H. F. **(2013)**. Toxicity assessment of anaerobic digestion intermediates and antibiotics in pharmaceutical wastewater by luminescent bacterium. *Journal of Hazardous Materials*, *246*, 319-323.

Karthikeyan, K. G. & Meyer, M. T. **(2006)**. Occurrence of antibiotics in wastewater treatment facilities in Wisconsin, USA. *Science of the Total Environment*, 361(1-3): 196-207.

Khan, E. A., Hafeez, A., & Ikram, A. **(2018)**. Situation analysis report on antimicrobial resistance in Pakistan-findings and recommendations for antibiotic use and resistance. Internet]. The Global Antibiotic Resistance Partnership (GARP), Pakistan.[cited 2018 Mar 19]. Available from: https://www. cddep. org/publications/garp-pakistan-situation-analysis.

Khan, G.A., Berglund, B., Khan, K.M., Lindgren, P-E., & Fick, J. **(2013).** Occurrence and abundance of antibiotics and resistance genes in rivers, canal and near drug formulation facilities – A study in Pakistan. *PLoS ONE*, 8(6).

Kimosop, S. J., Getenga, Z. M., Orata, F., Okello, V. A., & Cheruiyot, J. K. **(2016)**. Residue levels and discharge loads of antibiotics in wastewater treatment plants (WWTPs), hospital lagoons, and rivers within Lake Victoria Basin, Kenya. *Environmental Monitoring and Assessment, 188*(9), 532.

Klein, E. Y., Van Boeckel, T. P., Martinez, E. M., Pant, S., Gandra, S., Levin, S. A., & Laxminarayan, R. **(2018).** Global increase and geographic convergence in antibiotic consumption between 2000 and 2015. *Proceedings of the National Academy of Sciences*, *115*(15), E3463-E3470.

K'oreje, K. O., Demeestere, K., De Wispelaere, P., Vergeynst, L., Dewulf, J., & Van Langenhove, H. **(2012)**. From multi-residue screening to target analysis of pharmaceuticals in water: development of a new approach based on magnetic sector mass spectrometry and application in the Nairobi River Basin, Kenya. *Science of the Total Environment, 437,* 153–164.

Kovalova, L., Siegrist, H., von Gunten, U., Eugster, J., Hagenbuch, M., Wittmer, A., Moser, R. & McArdell, C.S. **(2013)** Elimination of micropollutants during post-treatment of hospital wastewater with powdered activated carbon, ozone, and UV. *Environmental Science & Technology*, 47(14), 7899-7908.

Kuang, Y., Wang, Q., Chen, Z., Megharaj, M., & Naidu, R., **(2013)**. Heterogeneous Fenton-like oxidation of monochlorobenzene using green synthesis of iron nanoparticles. *Journal of Colloid and Interface Science*, 410, 67–73.

Kumar, K., Gupta, S. C., Chander, Y., & Singh, A. K. **(2005)**. Antibiotic use in agriculture and its impact on the terrestrial environment. *Advances in Agronomy, 87*, 1-54.

Kumar, P. S., Vincent, C., Kirthika, K., & Kumar, K. S. **(2010).** Kinetics and equilibrium studies of Pb^{2+} in removal from aqueous solutions by use of nano-silversol-coated activated carbon. *Brazilian Journal of Chemical Engineering*, *27*(2), 339-346.

Lamastra, L., Suciu, N. A., & Trevisan, M. **(2018)**. Sewage sludge for sustainable agriculture: contaminants' contents and potential use as fertilizer. *Chemical and Biological Technologies in Agriculture*, *5*(1), 1-6.

Langmuir, I. **(1916)**. The constitution and fundamental properties of solids and liquids. Part I. solids, *Journal of American Chemical Society*. 38 (11), 2221–2295.

Larsson, D. J., de Pedro, C., & Paxeus, N. **(2007)**. Effluent from drug manufactures contains extremely high levels of pharmaceuticals. *Journal of Hazardous Materials*, *148*(3), 751-755.

Lee, T.-H., Ng, C., Chen, H., Yi, X. Z., Koh, T. H., & Barkham, T. M. S., **(2016)**. Occurrences and characterization of antibiotic-resistant bacteria and genetic determinants of hospital wastewater in a tropical country. *Antimicrobial Agents and Chemotherapy, 60*, 7449–7456.

Leng, L., Wei, L., Xiong, Q., Xu, S., Li, W., Lv, S., & Zhou, W. **(2020)**. Use of microalgae-based technology for the removal of antibiotics from wastewater: A review. *Chemosphere, 238*, 124680.

Li J, Ng DHL, Ma R, Zuo M, & Song., P. **(2017)** Eggshell membrane derived $MgFe_2O_4$ for pharmaceutical antibiotics removal and recovery from water. *Chemical Engineering Research and Design,* 126, 123–133.

Li, S., Wang, W., Liu, Y., & Zhang, W. X. **(2014).** Zero-valent iron nanoparticles (nZVI) for the treatment of smelting wastewater: a pilot-scale demonstration. *Chemical Engineering Journal*, *254*, 115-123.

Lien, L. T. Q., Hoa, N. Q., Chuc, N. T. K., Thoa, N. T. M., Phuc, H. D., & Diwan, T., **(2016)**. Antibiotics in wastewater of a rural and an urban hospital before and after wastewater treatment, and the relationship with antibiotic use-a one year study from Vietnam. *International Journal of Environmental Research and Public Health, 13*, 588–600.

Lin, Z., Weng, X., Owens, G., & Chen, Z. **(2020)**. Simultaneous removal of Pb (II) and rifampicin from wastewater by iron nanoparticles synthesized by a tea extract. *Journal of Cleaner Production*, *242*, 118476.

Lofrano, G., Pedrazzani, R., Libralato, G., & Carotenuto, M. **(2017)**. Advanced oxidation processes for antibiotics removal: a review. *Current Organic Chemistry*, *21*(12), 1054-1067.

Lonappan, L., Pulicharla, R., Rouissi, T., Brar, S. K., Verma, M., Surampalli, R. Y., & Valero, J. R. **(2016)**. Diclofenac in municipal wastewater treatment plant: quantification using laser diode thermal desorption-atmospheric pressure chemical ionization-tandem mass spectrometry approach in comparison with an established liquid chromatography-electrospray ionization–tandem mass spectrometry method. *Journal of Chromatography A*, *1433*, 106-113.

Loulidi, I., Boukhlifi, F., Ouchabi, M., Amar, A., Jabri, M., Kali, A., & Aziz, F. **(2020)**. Adsorption of crystal violet onto an agricultural Waste residue: Kinetics, isotherm, thermodynamics, and mechanism of adsorption. *The Scientific World Journal*, *2020*.

Matamoros, V., & Salvadó, V. **(2013)**. Evaluation of a coagulation/flocculation-lamellar clarifier and filtration-UV-chlorination reactor for removing emerging contaminants at full-scale wastewater treatment plants in Spain. *Journal of Environmental Management*, *117*, 96-102.

Mazzetti, L., & Thistlethwaite, P.J. **(2002)**. Raman spectra and thermal transformations of ferrihydrite and schwertmannite. *Journal of Raman Spectroscopy*. 33, 104–111. https://doi.org/ 10.1002/jrs.830.

Mezenner, N.Y., & Bensmaili, A. **(2009).** Kinetics and thermodynamic study of phosphate adsorption on iron hydroxide-eggshell waste. *Chemical Engineering Journal*, 147, 87e96. https://doi.org/10.1016/j.cej.2008.06.024.

Mohapatra, S., Huang, C. H., Mukherji, S., & Padhye, L. P. **(2016)**. Occurrence and fate of pharmaceuticals in WWTPs in India and comparison with a similar study in the United States. *Chemosphere*, *159*, 526-535.

Moraru, R., Pourcher, A. M., Jadas-Hecart, A., Kempf, I., Ziebal, C., Kervarrec, M., & Dabert, P. **(2012)**. Changes in concentrations of fluoroquinolones and of ciprofloxacin resistant Enterobacteriaceae in chicken feces and manure stored in a heap. *Journal of Environmental Quality*, *41*(3), 754-763.

Mouzam, M. I., Dehghan, M. H. G., Asif, S., Sahuji, T., & Chudiwal, P. **(2011)**. Preparation of a novel floating ring capsule-type dosage form for stomach specific delivery. *Saudi Pharmaceutical Journal*, *19*(2), 85-93.

Nawaz, M., Sliman, Y., Ercan, I., Lima-Tenório, M. K., Tenório-Neto, E. T., Kaewsaneha, C., & Elaissari, A. **(2019)**. Magnetic and pH-responsive magnetic nanocarriers. In *Stimuli Responsive Polymeric Nanocarriers for Drug Delivery Applications* (pp. 37-85). Woodhead Publishing.

Orwa, C., Mutua, A., Kindt, R., Jamnadass, R., & Anthony, S**. (2009)**. Agroforestree Database: a tree reference and selection guide version 4.0. *World Agroforestry Centre, Kenya*, *15*.

Pathak, A., Nowell, R. W., Wilson, C. G., Ryan, M. J., & Barraclough, T. G. **(2020).** Comparative genomics of Alexander Fleming's original Penicillium isolate (IMI 15378) reveals sequence divergence of penicillin synthesis genes. *Scientific Reports*, *10*(1), 1-10.

Peng, X., Ou, W., Wang, C., Wang, Z., Huang, Q., Jin, J., & Tan, J. **(2014)**. Occurrence and ecological potential of pharmaceuticals and personal care products in groundwater and reservoirs in the vicinity of municipal landfills in China. *Science of the Total Environment, 490*, 889–898.

Phoon, B. L., Ong, C. C., Saheed, M. S. M., Show, P. L., Chang, J. S., Ling, T. C., & Juan, J. C. **(2020)**. Conventional and emerging technologies for removal of antibiotics from wastewater. *Journal of Hazardous Materials*, *400*, 122961.

Pina, B., Bayona, J. M., Christou, A., Fatta-Kassinos, D., Guillon, E., Lambropoulou, D., & Sayen, S. **(2020)**. On the contribution of reclaimed wastewater irrigation to the potential exposure of humans to antibiotics, antibiotic resistant bacteria and antibiotic resistance genes–NEREUS COST Action ES1403 position paper. *Journal of Environmental Chemical Engineering*, *8*(1), 102131.

Pompeu, D.R., Larondelle, Y., Rogez, H., Abbas, O., Pierna, J.A., & Baeten, V. **(2018)**. Characterization and discrimination of phenolic compounds using Fourier transform Raman spectroscopy and chemometric tools. *Biotechnology, Agronomy, Society and Environment*. 22, 13–28.

Pouretedal, H. R., & Sadegh, N. **(2014).** Effective removal of amoxicillin, cephalexin, tetracycline and penicillin G from aqueous solutions using activated carbon nanoparticles prepared from vine wood. *Journal of Water Process Engineering*, *1*, 64-73.

Rana, A., Yadav, K., & Jagadevan, S. **(2020)**. A comprehensive review on green synthesis of nature-inspired metal nanoparticles: Mechanism, application and toxicity. *Journal of Cleaner Production*, 122880.

Rehman, M. S. U., Rashid, N., Ashfaq, M., Saif, A., Ahmad, N., & Han, J. I. **(2015)**. Global risk of pharmaceutical contamination from highly populated developing countries. *Chemosphere*, *138*, 1045-1055.

Report on Pakistan pharmaceutical industry. **(2017).** Pakistan research institute of market economy and Pakistan pharmaceutical manufacturers association.

Rezaei, F., & Vione, D., **(2018)**. Effect of pH on zero valent Iron performance in heterogeneous Fenton and fenton-like processes: a review. *Molecules*, 23, 3127. https://doi.org/10. 3390/molecules23123127.

Rodriguez, D. C., Ahammad, Z. S., Penuela, G. A., & Graham, D. W. **(2020)**. Effect of β-lactamases associated to the resistance of β-lactam antibiotics on the treatment of wastewater. *Journal of Environmental Chemical Engineering*, *8*(1), 102247.

Rodriguez-Mozaz, S., Chamorro, S., Marti, E., Huerta, B., Gros, M., Sànchez-Melsió, A., & Balcázar, J. L. **(2015)**. Occurrence of antibiotics and antibiotic resistance genes in hospital and urban wastewaters and their impact on the receiving river. *Water Research*, *69*, 234-242.

Rout, P. R., Zhang, T. C., Bhunia, P., & Surampalli, R. Y. **(2021)**. Treatment technologies for emerging contaminants in wastewater treatment plants: A review. *Science of the Total Environment*, *753*, 141990.

Sabri, N. A., van Holst, S., Schmitt, H., van der Zaan, B. M., Gerritsen, H. W., Rijnaarts, H. H. M., & Langenhoff, A. A. M. **(2020)**. Fate of antibiotics and antibiotic resistance genes during conventional and additional treatment technologies in wastewater treatment plants. *Science of the Total Environment*, *741*, 140199.

Saif, S., Tahir, A., & Chen, Y. **(2016).** Green synthesis of iron nanoparticles and their environmental applications and implications. *Nanomaterials*, *6*(11), 209.

Saini, R. K., Sivanesan, I., & Keum, Y. S. **(2016)**. Phytochemicals of *Moringa oleifera*: a review of their nutritional, therapeutic and industrial significance. *3 Biotech*, *6*(2), 1-14.

Salem, S. S., & Fouda, A. **(2020)**. Green synthesis of metallic nanoparticles and their prospective biotechnological applications: an overview. *Biological Trace Element Research*, 199(1)344-370.

Schmidt, M., Masson, A., Cheng, H.P., & Brchignac, C. **(2015).** Physisorption and chemisorption on silver clusters. *ChemPhysChem* 16, 855-865.

Segura, P. A., Takada, H., Correa, J. A., El Saadi, K., Koike, T., Onwona-Agyeman, S., et al. **(2015)**. Global occurrence of anti-infectives in contaminated surface waters: Impact of income inequality between countries. *Environment International, 80,* 89–97.

Shirzad Siboni, M., Samadi, M. T., Azizian, S., Maleki, A., & Zarrabi, M. **(2011).** Removal of chromium by using of adsorption onto strong base anion resin: study of equilibrium and kinetic. *Journal of Water and Wastewater*, *22*(3), 10-18.

Shukla, A., Zhang, Y. H., Dubey, P., Margrave, J. L., & Shukla, S. S. **(2002).** The role of sawdust in the removal of unwanted materials from water. *Journal of Hazardous Materials*, *95*(1-2), 137-152.

Sim, W. J., Lee, J. W. and Oh, J. E. **(2010)**. Occurrence and fate of pharmaceuticals in wastewater treatment plants and rivers in Korea. *Environmental Pollution.* 158(5): 1938-1947.

Sim, W. J., Lee, J. W., Lee, E. S., Shin, S. K., Hwang, S. R., & Oh, J. E. **(2011)**. Occurrence and distribution of pharmaceuticals in wastewater from households, livestock farms, hospitals and pharmaceutical manufactures. *Chemosphere*, *82*(2), 179-186.

Sreelatha, S., & Padma, P. R. **(2009)**. Antioxidant activity and total phenolic content of *Moringa oleifera* leaves in two stages of maturity. *Plant Foods for Human Nutrition*, *64*(4), 303-311.

Stan, M., Lung, I., Soran, M. L., Leostean, C., Popa, A., Stefan, M.,& Porav, A. S. **(2017).** Removal of antibiotics from aqueous solutions by green synthesized magnetite nanoparticles with selected agro-waste extracts. *Process Safety and Environmental Protection*, *107*, 357-372.

Sun, Y., Yang, S., Chen, Y., Ding, C., Cheng, W. & Wang, X. **(2015)** Adsorption and desorption of U(VI) on functionalized graphene oxides: A combined experimental and theoretical study. *Environmental Science & Technology.* 49(7), 4255-4262.

Swann, R. L., Laskowski, D. A., McCall, P. J., Vander Kuy, K., & Dishburger, H. J. **(1983)**. A rapid method for the estimation of the environmental parameters octanol/water partition coefficient, soil sorption constant, water to air ratio, and water solubility. *Residue Reviews*, 17-28.

Tan, F., Liu, M., & Ren, S. **(2017)**. Preparation of polydopamine-coated graphene oxide/Fe_3O_4 imprinted nanoparticles for selective removal of fluoroquinolone antibiotics in water. *Scientific Reports*, *7*(1), 1-9.

Torniainen, K., Tammilehto, S., & Ulvi, V. **(1996)**. The effect of pH, buffer type and drug concentration on the photodegradation of ciprofloxacin. *International Journal of Pharmaceutics*, *132*(1-2), 53-61.

TRTA II Programme: Extended - TRTA Pakistan. **(2020)**.

Turku, I., Sainio, T., & Paatero, E. **(2007).** Thermodynamics of tetracycline adsorption on silica. *Environmental Chemistry Letters*, *5*(4), 225-228.

Vongsak, B., Sithisarn, P., Mangmool, S., Thongpraditchote, S., Wongkrajang, Y., & Gritsanapan, W. **(2013).** Maximizing total phenolics, total flavonoids contents and antioxidant activity of *Moringa oleifera* leaf extract by the appropriate extraction method. *Industrial Crops and Products*, *44*, 566-571.

Wallaice, S. C., Gahan, L. R., Charles, B. G., Hambley, T. W., & Duckworth, P. A. **(1996).** Copper (II) complexes of the fluoroquinolone antimicrobial ciprofloxacin. Synthesis, X-ray structural characterization, and potentiometric study. *Journal of Inorganic Biochemistry*, *62*(1), 1-16.

Walsh, C. **(2003)**. Antibiotics: actions, origins, resistance. *American Society for Microbiology (ASM)*.

Wang, Y., Wang, X., Li, M., Dong, J., Sun, C., & Chen, G. **(2018)**. Removal of pharmaceutical and personal care products (PPCPs) from municipal wastewater with integrated membrane systems, MBR-RO/NF. *International Journal of Environmental Research and Public Health*, *15*(2), 269.

Weber, W.J., Morris, J.C., **(1963).** Kinetics of adsorption on carbon from solution. *Journal of Sanitation Engineering Division*. 89, 31e60.

Weng, X., Huang, L., Chen, Z., Megharaj, M., & Naidu, R., **(2013).** Synthesis of iron-based nanoparticles by green tea extract and their degradation of malachite. *Industrial Crop Production*. 51, 342–347.

Weng, X., Owens, G., & Chen, Z. **(2020)**. Synergetic adsorption and Fenton-like oxidation for simultaneous removal of ofloxacin and enrofloxacin using green synthesized Fe NPs. *Chemical Engineering Journal*, *382*, 122871.

Worch, E. **(2012)**. Adsorption technology in water treatment: Fundamentals. *Processes, and Modeling*, 1-332.

Wu, J., Lin, Z., Weng, X., Owens, G., & Chen, Z. **(2020)**. Removal mechanism of mitoxantrone by a green synthesized hybrid reduced graphene oxide@ iron nanoparticles. *Chemosphere*, *246*, 125700.

Wu, Q., Li, Z., Hong, H., Yin, K., & Tie, L. **(2010).** Adsorption and intercalation of ciprofloxacin on montmorillonite. *Applied Clay Science*, *50*(2), 204-211.

Wu, Y. **(2017)**. Investigation of adsorption and absorption mechanisms during copper (II) removal by periphyton. *Periphyton: Functions and Application in Environmental Remediation. Elsevier, Boston,* 303-321.

Xing, Z., Zhang, J., Cui, J., Yin, J., Zhao, T., Kuang, J., & Zhou, W. **(2018)**. Recent advances in floating TiO2-based photocatalysts for environmental application. *Applied Catalysis B: Environmental*, *225*, 452-467.

Xu, W., Zhang, G., Li, X., Zou, S., Li, P., Hu, Z. & Li, J. **(2007)**. Occurrence and elimination of antibiotics at four sewage treatment plants in the Pearl River Delta (PRD), South China. *Water Research.* 41(19): 4526-4534.

Yan, B., Niu, C. H., & Wang, J. **(2017)**. Kinetics, electron-donor-acceptor interactions, and site energy distribution analyses of norfloxacin adsorption on pretreated barley straw. *Chemical Engineering Journal*, *330*, 1211-1221.

Yang, J., Lu, Z. Y., Hu, J. C. & Gu, X. S. **(1997)**. Advances in biological treatment processes of antibiotic production wastewater. *Environmental Science* (Chinese). 18(3): 83-85

Yao, L., Wang, Y., Tong, L., Deng, Y., Li, Y., Gan, Y., Guo, W., Dong, C., Duan, Y., & Zhao, K. **(2017)**. Occurrence and risk assessment of antibiotics in surface water and groundwater from different depths of aquifers: A case study at Jianghan Plain, central China. *Ecotoxicology and Environmental Safety*. *135*, 236–242.

Yasojima, M., Nakada, N., Komori, K., Suzuki, Y. & Tanaka, H. **(2006)**. Occurrence of levofloxacin, clarithromycin and azithromycin in wastewater treatment plant in Japan. *Water Science and Technology.* 53(11): 227-233.

Yazdani, F., & Seddigh, M. **(2018).** Magnetite nanoparticles synthesized by co-precipitation method: The effects of various iron anions on specifications. *Materials Chemistry and Physics*, *184*, 318-323.

Yoon, S., Lee, C., Park, J., Kim, J., Kim, S., Lee, S., & Choi, J., **(2014)**. Kinetic, equilibrium and thermodynamic studies for phosphate adsorption to magnetic iron oxide nanoparticles. *Chemical Engineering Journal,* 236, 341-347.

Yu, F., Li, Y., Han, S., & Ma, J. **(2016)**. Adsorptive removal of antibiotics from aqueous solution using carbon materials. *Chemosphere*, *153*, 365-385.

Zafar, R., Bashir, S., Nabi, D., & Arshad, M. **(2021).** Occurrence and quantification of prevalent antibiotics in wastewater samples from Rawalpindi and Islamabad, Pakistan. *Science of the Total Environment*, 142596.

Zhang, C., Yu, Z., Zeng, G., Huang, B., Dong, H., Huang, J., Yang, Z., Wei, J., Hu, L., Zhang, Q., **(2016).** Phase transformation of crystalline iron oxides and their adsorption abilities for Pb and Cd. *Chemical Engineering Journal*. 284, 247-259.

Zhang, R., Zhang, G., Zheng, Q., Tang, J., Chen, Y., Xu, W., et al. **(2012)**. Occurrence and risks of antibiotics in the Laizhou Bay, China: Impacts of River Discharge. *Ecotoxicology and Environmental Safety, 80*, 208–215.

Zhang, Y., Yang, Z., Xiang, Y., Xu, R., Zheng, Y., Lu, Y., & Xiong, W. **(2020)**. Evolutions of antibiotic resistance genes (ARGs), class 1 integron-integrase (intI1) and potential hosts of ARGs during sludge anaerobic digestion with the iron nanoparticles addition. *Science of the Total Environment*, *724*, 138248.

Zhou, A., Zhu, C., Chen, W., Wan, J., Tao, T., Zhang, T.C., & Xie, P. **(2018**). Phosphorus recovery from water by lanthanum hydroxide embedded interpenetrating network poly (vinyl alcohol)/sodium alginate hydrogel beads. *Colloids and Surface. A Physicochemical and Engineering Aspect.* 554, 237-244.